

Structural Features of Tetraazathiapentalenes Fused with Pyrimidine and/or Pyridine Rings. Experimental Evaluation of the Nature of Hypervalent N–S–N Bond by Restricted Internal Rotation of the Pyrimidine Ring

Katsuo Ohkata, Minoru Ohsugi, Kazuhiro Yamamoto, Mika Ohsawa, and Kin-ya Akiba*

Contribution from the Department of Chemistry, Faculty of Science, Hiroshima University, 1-3-1 Kagamiyama, Higashi-Hiroshima 739, Japan

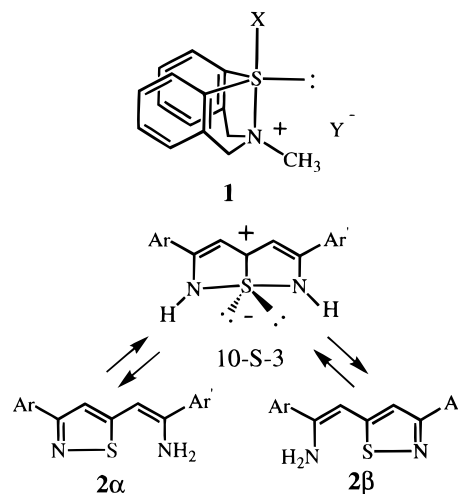
Received August 1, 1995. Revised Manuscript Received May 4, 1996[⊗]

Abstract: A series of neutral (**8–10**), monomethylated (**12–14**), and dimethylated (**17**) 10-S-3 sulfuranes, derivatives of tetraazathiapentalenes fused with pyrimidine and/or pyridine ring, were prepared. These molecules are planar, and bond energies of the hypervalent N–S–N bond were evaluated by the temperature dependent restricted rotation of the pyrimidine ring caused by cleavage of one of the S–N bonds. The bond length is longer, and the energy is lower for the S–N bond fused with more electron-withdrawing heterocycles.

Introduction

A large number of organosulfur compounds are known, where conformations are considerably influenced by intramolecular sulfur–nitrogen (or oxygen) interactions.¹ Such effects of intermolecular as well as intramolecular attractive interaction (besides the routinely “discussed” hydrogen bonding) on the conformations of biological macromolecules are a growing field of study.² In these molecules the S···N or S···O nonbonded distances are significantly shorter than the sum of the corresponding van der Waals radii (3.35 or 3.32 Å). In the preceding papers, we showed that the most stable conformation of eight-membered ring in benzothiazocine derivatives (**1**) containing sulfur and nitrogen atoms at 1,5-position is a twist-boat form rather than a boat-chair form due to N–S intramolecular hypervalent bond formation (Chart 1).^{3a} X-ray structural analysis of these compounds confirmed the transannular bond formation between the sulfur and the nitrogen.^{3b} The structural features (bond distances and bond angles) and ¹H and ¹⁵N NMR chemical shifts for the methylammonium group vary in the expected manner with the electronegativity of the apical ligand (X).^{3c} The chemical shifts are linearly correlated with σ_1 values for the substituent X. Martin and his co-workers also showed that the charge distribution in unsymmetrically substituted

Chart 1



hypervalent species is experimentally demonstrated through spectroscopic methods (NMR and IR).⁴

In the last two decades, we have investigated several examples of ring-transformation (“bond switching”: $2\alpha \rightleftharpoons 2\beta$) via hypervalent sulfurane in 5-aminovinylisothiazole **2** and its derivatives (Chart 1).⁵ Many examples of isolable 10-S-3 species are known, perhaps the most numerous examples of 10-S-3 species are thiathiophthen (**3a**) and its analogs **3b**.^{1,6} The bond polarization in hypervalent sulfur compounds is also reflected in ground state structures. In the series of 10-S-3 sulfurane species, the bond distances in three-center four-electron bond vary with the difference of electronegativity between the two apical ligands.¹ The changing of bond

[⊗] Abstract published in *Advance ACS Abstracts*, June 15, 1996.

(1) (a) Leung, F.; Nyburg, S. C. *Can. J. Chem.* **1971**, *49*, 167. (b) Hansen, L. K.; Hordvik, A.; Saethre, L. J. *Organic Sulfur Chemistry*; Stirling, C. J. M., Ed.; Butterworths: London and Boston, 1975; pp 1–17. (c) Gleiter, R.; Gyax, R. *Top. Curr. Chem.* **1976**, *63*, 49. (d) Lozac’h, N. *Adv. Heterocyclic Chem.* **1971**, *13*, 161. (e) Gleiter, R.; Spanget-Larsen, J. *Top. Curr. Chem.* **1979**, *86*, 139. (f) Musher, J. I. *Angew. Chem., Int. Ed. Engl.* **1969**, *8*, 54. (g) Hayes, R. A.; Martin, J. C. *Organic Sulfur Chemistry: Theoretical and Experimental Advances*; Bernardi, F., Csizmadia, I. G., Mangini, A., Eds.; Elsevier Scientific Publishing Co.: Amsterdam, 1985; p 408. (h) Kucsman, A.; Kapovits, I. *Organic Sulfur Chemistry: Theoretical and Experimental Advances*; Bernardi, F., Csizmadia, I. G., Mangini, A., Eds.; Elsevier Scientific Publishing Co.: Amsterdam, 1985; p 191.

(2) (a) Goldstein, B. M.; Takusagawa, F.; Berman, H. M.; Srivastava, P. C.; Robins, R. K. *J. Am. Chem. Soc.* **1983**, *105*, 7416. (b) Burling, F. T.; Goldstein, B. M. *J. Am. Chem. Soc.* **1992**, *114*, 2313. (c) Barton, D. H. R.; Hall, M. B.; Lin, Z.; Parekh, S. I.; Reibenspies, J. *J. Am. Chem. Soc.* **1993**, *115*, 5056.

(3) (a) Akiba, K.-y.; Takee, K.; Ohkata, K.; Iwasaki, F. *J. Am. Chem. Soc.* **1983**, *105*, 6965. (b) Akiba, K.-y.; Takee, K.; Shimizu, Y.; Ohkata, K. *J. Am. Chem. Soc.* **1986**, *108*, 6320. (c) Ohkata, K.; Ohnishi, M.; Yoshinaga, K.; Akiba, K.-y.; Rongione, J. C.; Martin, J. C. *J. Am. Chem. Soc.* **1991**, *113*, 9270.

(4) (a) Lau, P. H. W.; Martin, J. C. *J. Am. Chem. Soc.* **1978**, *100*, 7077. (b) Livant, P.; Martin, J. C. *J. Am. Chem. Soc.* **1977**, *99*, 5761. (c) Lam, W. Y.; Duesler, E. N.; Martin, J. C. *J. Am. Chem. Soc.* **1981**, *103*, 127. (5) (a) Akiba, K.-y.; Kobayashi, T.; Arai, S. *J. Am. Chem. Soc.* **1979**, *101*, 5857. (b) Akiba, K.-y.; Kashiwagi, K.; Ohyama, Y.; Yamamoto, Y.; Ohkata, K. *J. Am. Chem. Soc.* **1985**, *107*, 2721.

(6) (a) The N–X–L designation was proposed by J. C. Martin *et al.*: X, central atom; N, formal valence-shell electrons about an X; L, the number of ligands. Perkins, C. W.; Martin, J. C.; Arduengo, A. J.; Algeria, A.; Kochi, J. K. *J. Am. Chem. Soc.* **1980**, *102*, 7753. (b) Arndt, F.; Nachtweg, P.; Puscher, J. *Chem. Ber.* **1925**, *58*, 1633. (c) Bezzi, S.; Mammi, M.; Garbuglio, C. *Nature (London)* **1958**, *182*, 247. (d) Pfister-Guillouzo, G. *Bull. Soc. Chim. Fr.* **1958**, 1316.

Chart 2

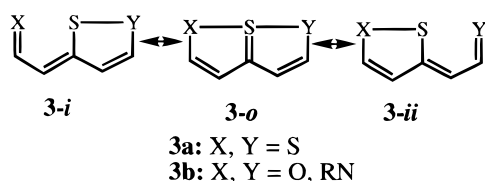


Chart 3

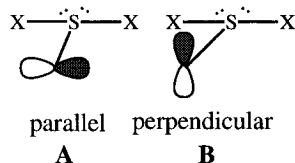
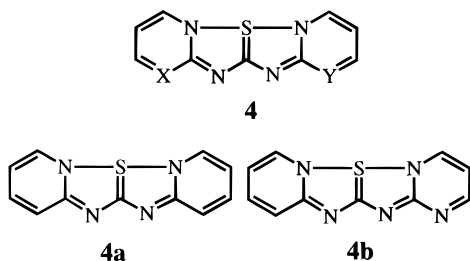


Chart 4

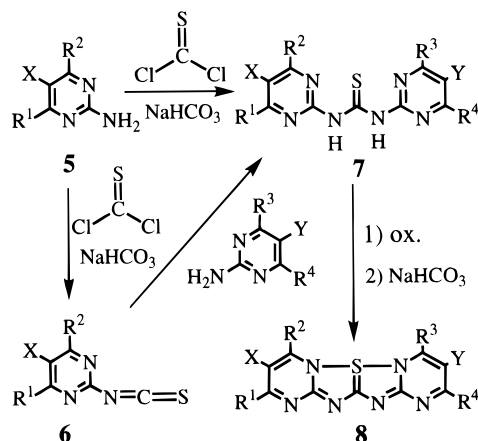


distances can be rationalized by considering the “no-bond” resonance structures as shown in Chart 2.

Burgess and Arduengo calculated the possible orientations for the equatorial π -acceptor ligand in most of 10-S-3 species.⁷ Both the parallel (**A**) and perpendicular (**B**) π -acceptor interactions with the hypervalent bond were found to be stabilizing (Chart 3). Interaction with the sulfur lone pair stabilized geometry (**B**) with respect to **A** by ca. 12 kcal/mol.

According to this information, tetraazathiapentalenes (**4**) fused with electron-withdrawing heterocycles (pyrimidine, pyridine, etc.) seem to be one of the ideal systems for formation of a stable 10-S-3 hypervalent sulfurane (Chart 4). Furthermore, the tridentate ligand in this system must be excellent in achieving planarity and rigidity of the molecule. Fortunately, some systems such as **4a** and **4b** fused with pyridine and/or pyrimidine had been synthesized by Harris in 1972 and by Potts in 1974, independently.⁸ However, they have described neither discussions about the chemical behavior nor the temperature dependence in the ¹H NMR spectra of these compounds. The 10-S-3 sulfuranes described here are expected to be planar in which the π -system can adopt effective orbital overlap and electron delocalization. The planar structure would support not only conjugative stabilization but also N–S–N hypervalent attractive interaction rather than the van der Waals repulsion between the heteroatoms (S and N). Therefore, cleavage of one of the hypervalent N–S–N bond to give an N–S bond in thiadiazolo ring will partly lose such a stabilization in the transition state of the internal rotation of the pyrimidine ring. Although there are many theoretical investigations on hypervalent bonding of 10-S-3 sulfuranes,⁹ there has been only a few experimental efforts to evaluate the bond strength.^{10,11} We now discuss both the structural features and the experimental evaluation of bond

Scheme 1



energy and reactivity of hypervalent bond in the 10-S-3 sulfuranes (**8**, **9**, **12**, and **17**) fused with pyrimidine rings such as **4b**.

Results and Discussion

Preparation of Tetraazathiapentalene Derivatives and Related Compounds. Tetraazathiapentalenes (**8**–**10**) fused with pyrimidine and/or pyridine were prepared by the modified method described by Harris and Potts.⁸ Treatment of 2-aminopyrimidine derivatives **5a**–**c** with thiophosgene in the presence of NaHCO₃ afforded the corresponding symmetric thioureas **7a**–**c** as shown in Scheme 1. The other unsymmetric dipyrimidylthioureas **7d**–**i** were obtained by coupling of **5** with isothiocyanates **6a**–**c**. Oxidation of the thioureas **7a**–**i** with appropriate oxidants (SO₂Cl₂, NBS, and NCS) gave the tetraazathiapentalene derivatives **8a**–**i** (10-S-3 system) fused with the two pyrimidine rings. The other thioureas (**7j**–**n**) were obtained by condensation of *S*-methyl dithiocarbamates (**6f**–**i**) with 2-aminopyrimidine derivatives **5a**,**e**, followed by oxidation to give **9a**–**e** and **9e'**. Bromination of **8a** with NBS afforded the dibromo-substituted compound **8c**. The related thiadiazolo- and dipyridyltetraazapentalene derivatives **9f** and **10** were also prepared by way of the corresponding thioureas (**7o** and **7p**).

In ¹H NMR spectra in CD₂Cl₂ at 0 °C, **8a** showed a singlet at δ 2.53 and a doublet at δ 2.66 with $J = 0.66$ Hz for the two nonequivalent methyl groups of the pyrimidine ring in which the chemical shifts were separated by 10.3 Hz ($\Delta\nu$) at 90 MHz, and the integral ratio of the two signals was 1:1. The symmetric dihalogeno sulfuranes **8b** and **8c** showed two singlets for methyl groups at slightly lower field relative to that of **8a** at 0 °C. On the other hand, the ¹H NMR spectra of monohalogenated substrates **8d**–**f** at 0 °C showed four signals assigned to each methyl group along with a quartet around δ 6.6 ($J = 0.66$ Hz) for the pyrimidine proton. One of the methyl signals coupled with the pyrimidine ring proton appeared as a clear doublet at δ 2.70 with a small coupling constant ($^4J = 0.66$ Hz for **8d**). According to both the coupling of heterocyclic protons ($Y = H$) and the coalescence temperature of each pair of the methyl signals as described below, the doublet signal and its counterpart were assigned to the methyl groups of the unhalogenated pyrimidine ring. In the ¹H NMR spectrum of **8g**–**i**, there were

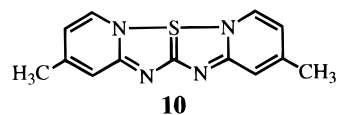
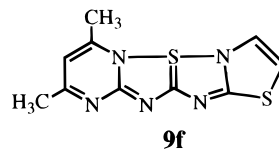
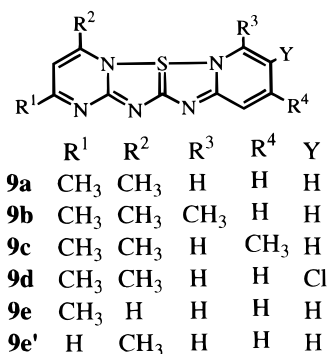
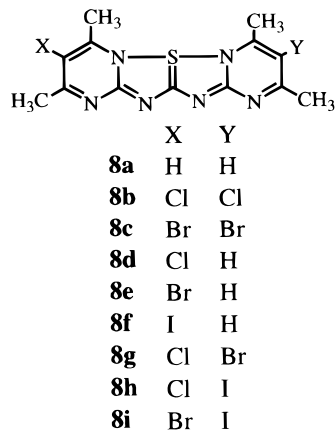
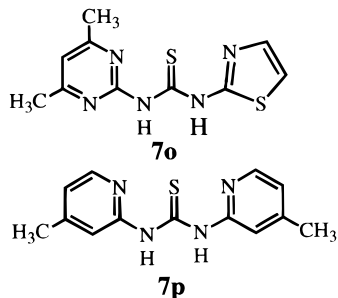
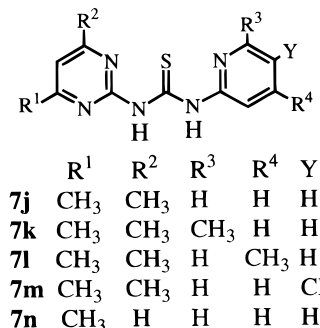
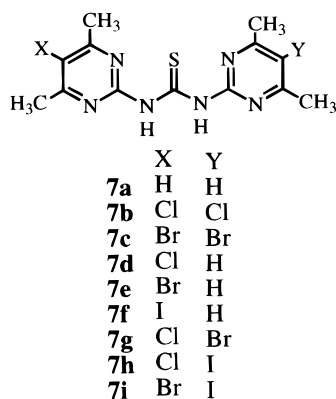
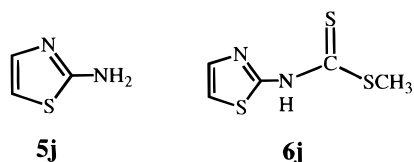
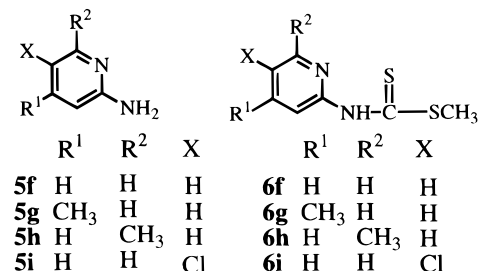
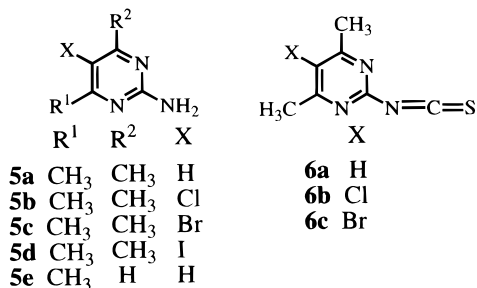
(10) L'abbe, G.; Van Meervelt, L.; Sabine, E.; Wim, D.; Suzanne, T. *J. Heterocycl. Chem.* **1992**, *29*, 1765.

(11) (a) Akiba, K.-y.; Ohsugi, M.; Iwasaki, H.; Ohkata, K. *J. Am. Chem. Soc.* **1988**, *110*, 5576. (b) Ohkata, K.; Ohsugi, M.; Kuwaki, T.; Yamamoto, K.; Akiba, K.-y. *Tetrahedron Lett.* **1990**, *31*, 1605. Ohkata, K.; Yamamoto, K.; Ohsugi, M.; Ohsawa, M.; Akiba, K.-y. *Heterocycles* **1994**, *38*, 1707. **8a**: 2,4,8,10-tetramethyl-6 λ^4 -pyrimido[1''',2''',3']-[1,2,4]-thiadiazolo[1',5':1,5][1,2,4]thiadiazolo[2,3-*a*]pyrimidine, the numbering of *Chem. Abstr.* is used throughout this paper except X-ray data and AM1 calculations.

(7) Arduengo III, A. J.; Burgess, E. M. *J. Am. Chem. Soc.* **1977**, *99*, 2376.

(8) (a) Harris, R. L. *N. Aust. J. Chem.* **1972**, *25*, 993. (b) Potts, K. T.; Kane, J. *J. Org. Chem.* **1974**, *39*, 3783.

(9) (a) Angyan, J. G.; Poirier, R. A.; Kucsman, A.; Csizmadia, I. G. *J. Am. Chem. Soc.* **1987**, *109*, 2237. (b) Lin, K. J.; Wang, Y. *J. Phys. Chem.* **1993**, *97*, 3176. (c) Minkin, V. I. *Pure Appl. Chem.* **1989**, *61*, 661.



of **8d** showed three signals assigned to each methyl group in which two methyl signals at δ 2.73 overlapped each other.

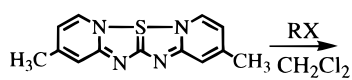
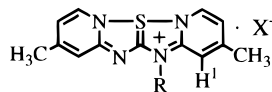
In ¹H NMR spectrum at ambient temperature (35 °C) in CDCl₃ solution, **9a** showed two methyl peaks at δ 2.54 and 2.68 (integral ratios 1:1, separated by 13.2 Hz ($\Delta\nu$) at 90 MHz) along with a sharp proton singlet at δ 6.54 for the pyrimidine ring and clearly separated multiplets at δ 6.8–8.4 for pyridine protons.

The ¹H NMR spectrum of **9e** and **9e'** at 10 °C showed two peaks at δ 2.62 and 2.77 (integral ratio 2:3, total 3H, separated by 13.5 Hz at 90 MHz) as monomethyl derivative. The two singlets coalesced at 45 °C, but the other signals for the heterocyclic ring protons remained unchanged. The singlet signal (δ 2.62) for the methyl hydrogens at higher magnetic field can be assigned to that of isomer **9e** on the basis of assignment for **8a**.

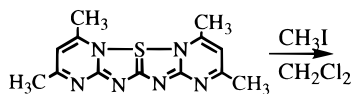
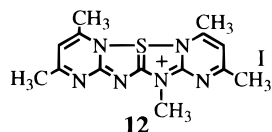
Comparisons of the ¹H NMR chemical shifts of the pyrimidine ring proton in **8a**, **8d**, **9a**, **9d**, and **12** reveal the influence by the electronic properties of the heterocycle on the other side in the 10-S-3 sulfurane. Thus, the signal at δ 6.62 of **8a** shifted downfield to δ 6.65 in **8d** by the chloro-substituent at the other side of the pyrimidine ring. There is observed the same tendency between **9a** (δ 6.59), **9d** (δ 6.59), and **12** (δ 7.30). The electronic effect must be transmitted mainly through the N–S–N hypervalent bond rather than the π -conjugation.

observed four singlets for **8g,i** or three singlets for **8h** which were arbitrarily assigned on the basis of the ¹H NMR chemical shift in **8d–f** where the methyl signals appeared at higher field in the following order: Cl > Br > I. The ¹H NMR spectrum

Scheme 2

**10**

11a: $R = CH_3$, $X = I$
11b: $R = CH_2CO_2Et$, $X = Br$

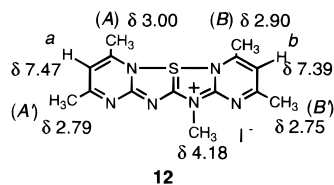
**8a****12**

Treatment of **10** with alkyl halides (CH_3I and $BrCH_2CO_2Et$) afforded the *N*-alkylated products **11a** (76%) and **11b** (88%), respectively. Regiochemistry of alkylation in **11b** was confirmed by NOE experiments in the 1H NMR spectrum. The NOED spectrum of **11b** showed an enhancement (11%) in the magnitude of the signal at δ 7.53 (H^1) at 1-position when the methylene signal of CH_2-CO_2Et at δ 5.49 was irradiated. This result indicates that alkylation (ethoxycarbonylmethylation) occurred exclusively at the nitrogen of 12(or 13)-position and not at 5(or 7)-position of **10**.

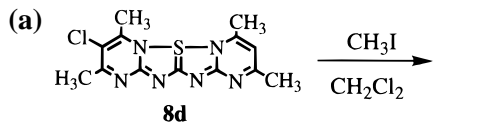
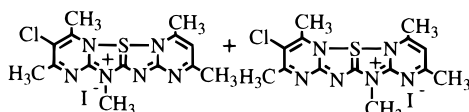
Reaction of **8a** with methyl iodide gave **12** (78%). In 1H NMR spectrum at 35 °C ($CDCl_3$), **12** shows a pair of singlets at δ 2.65, 2.73 and a pair of doublets at δ 3.03 ($J = 0.65$ Hz, 3H), 3.23 ($J = 0.66$ Hz, 3H) along with a singlet at δ 4.11 for the *N*- CH_3 group and a pair of quartet at δ 7.16 ($J = 0.65$ Hz, 1H), 7.30 ($J = 0.66$ Hz, 1H). Treatment of electronically unbalanced sulfuranes **8d** and **9a** with methyl iodide furnished a mixture of isomers, i.e., **13-N,F** and **14-N,F** in the product ratio of 2:1 and 9:1, respectively (Scheme 3, parts a and b).

It was very difficult to assign the methyl signals in the 1H NMR spectrum to the specific positions in the product **12** and to determine exactly the methylated positions in **13** and **14**. Therefore, **12-d₆**, **13-F**, and **14-N** were prepared by alternative routes as shown in Scheme 4, parts a and b. Reaction of 2-(methylamino)-4,6-dimethylpyrimidine-*d*₆ (**15-d₆**) with isothiocyanate **6a** gave the corresponding thiourea which was converted to **12-d₆** after oxidation with *N*-chlorosuccinimide. Figure 1 shows the assignment of 1H NMR spectrum for **12**. By the same procedure, reaction of **15** with **6b** and 2-isothiocyanatopyridine gave **13-F** and **14-N**, respectively. By comparison of the 1H NMR spectra of these compounds with those of the methylation products of **8d** and **9a**, the assignment of 1H NMR spectra was firmly established.

Then, the ratios between the regioisomers were determined by comparison of the integral values of the corresponding methyl signals as the following; i.e., **13-N:13-F** = 2:1; **14-N:14-F** = 9:1, respectively. Now, it is concluded that methylation of the tetraazathiapentalenes takes place mainly on the nitrogen at 13 position which is linked to the more electron-withdrawing heterocyclic ring. The result is contrary to the expectation based simply on the inductive effect of the starting heterocycle, but it can be realized by the greater stability of the positive charge endowed by the resonance structures.

**12**Figure 1. 1H NMR chemical shifts of **12** in CD_3OD .

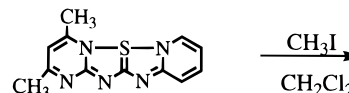
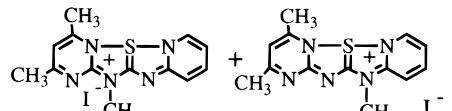
Scheme 3

**8d****13-N****13-F**

2

1

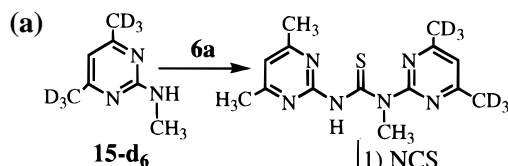
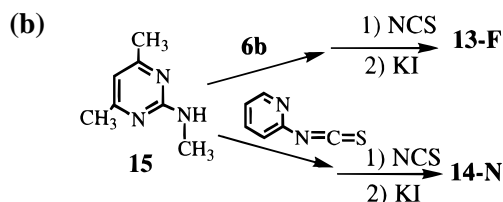
(b)

**9a****14-N****14-F**

9

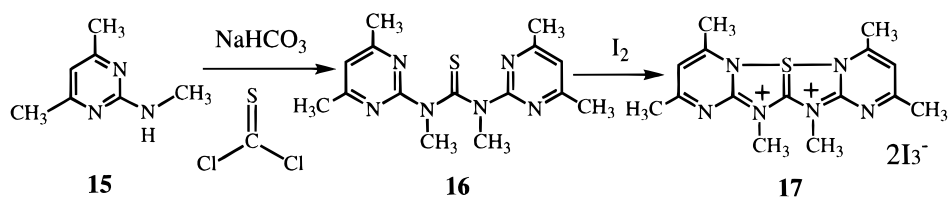
1

Scheme 4

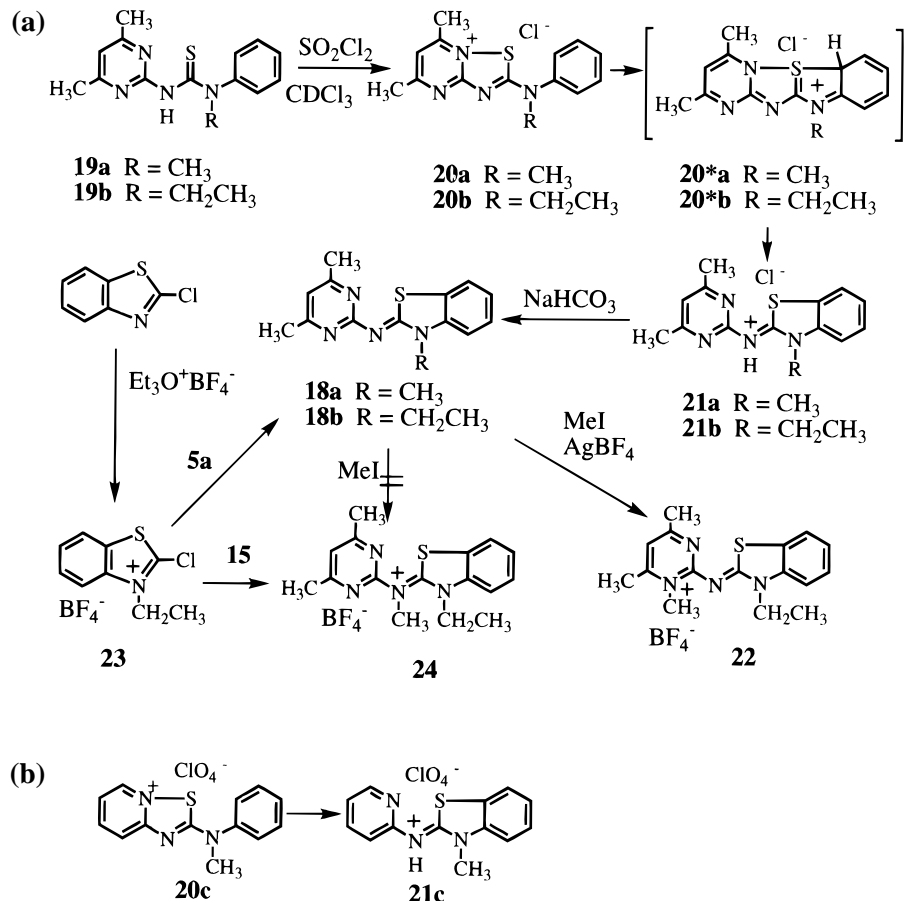
**15-d₆****12-d₆****15****13-F****14-N**

Reaction of 2-(methylamino)-4,6-dimethylpyrimidine (**15**) with thiophosgene in the presence of $NaHCO_3$ in CH_3CN gave *N,N'*-dimethylthiourea derivative **16** in 43% yield. Oxidation of **16** with 3 equiv of iodine in CH_2Cl_2 afforded the dicationic 10-*S*-3 sulfurane (**17**) as black brown crystals quantitatively (Scheme 5). This dicationic **17** could not be obtained by methylation of **12** with methyl iodide even in the presence of silver tetrafluoroborate. In 1H NMR spectrum at 35 °C (CD_3CN), **17** shows a pair of singlets at δ 2.83 (6H) and 2.99 (6H) along with a singlet at δ 4.57 for the *N*- CH_3 group and a singlet at δ 7.66 (2H) for the pyrimidine ring protons.

Scheme 5



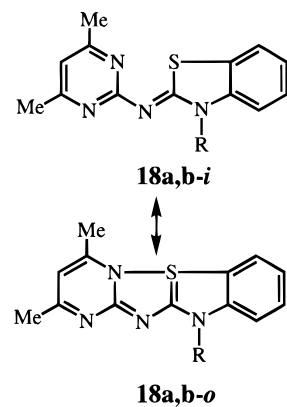
Scheme 6



Benzothiazoline derivatives (**18a,b**) were prepared by almost the same methodology described by Harris (Scheme 6, part a).^{8a} Oxidation of the corresponding thioureas **19a,b** with SO_2Cl_2 gave pyrimidothiazole derivatives (**20a,b**). In the ^1H NMR spectrum in $\text{DMSO}-d_6$, **20a** showed a singlet at δ 3.76 along with the other signals. The spectrum changed gradually into the other one which was assigned to that of **21a**. The result indicates that the initial product **20a** easily transformed the ring into benzothiazoline derivative **21a** at 40 °C. A half-life of the ring-transformation of **20a** was observed to be about 11 min, while that of **20c** into **21c** was about 40 min under the same conditions (Scheme 6, part b).^{8a} Treatment of the product (**21a,b**) with NaHCO_3 afforded **18a,b**. One (**18b**) of them was alternatively prepared by condensation of 2-chloro-3-ethylbenzothiazoline (**23**) with **5a**. In the ^1H NMR spectrum of **18b**, there are seen the characteristic signals at δ 2.54 (s, 6H) and 6.65 (s, 1H) for the pyrimidine ring along with the signals of the benzothiazoline moiety. Reaction of **18b** with methyl iodide did not afford **24** but *N*-methylated pyrimidine derivative (**22**), exclusively. The structure of **24** was definitely confirmed by an alternative preparation of **24** from **23** and **15**.

Since the pyrimidine side is more electronegative than the phenyl side, this large electronic imbalance between the two apical ligands results in almost exclusive contribution of the “no-bond” resonance form of **18a,b-i**, thus the two methyl

Scheme 7



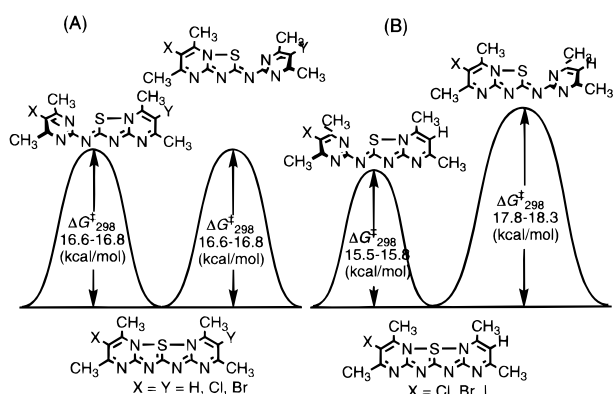
groups of the pyrimidine ring appear as a singlet (Scheme 7). Consequently, the N–S attractive interaction in **18**, if any, is so weak that methyl iodide attacked only the nitrogen of the pyrimidine ring to give **22**.

Evaluation of Hypervalent Bond Energy by Temperature Dependent ^1H NMR. Symmetric 10-S-3 Sulfurane. The two methyl signals of symmetric molecules, i.e., **8a–c**, coalesced at 45, 47, and 48 °C in CD_2Cl_2 , respectively. The exchange rate at the coalescence temperature (T_c) was calculated by using

Table 1. Kinetic Data for Restricted Rotation of **8**, **9**, and **12**

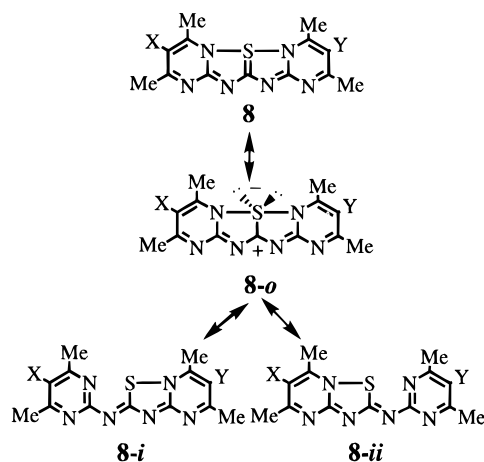
compd	X	Y	solvent ^a	T _c (°C)	Δν (Hz)	k _c (s ⁻¹)	ΔG _c [‡] (kcal/mol)	ΔG ₂₉₈ [‡] (kcal/mol)	ΔH [‡] (kcal/mol)	ΔS [‡] (eu)	
8a	H	H	A	44	12.5	27.8	16.6				
	H	H	B	45	10.3	22.9	16.7	16.6	15.9 ± 1.1	-2.4 ± 3.4	
8b	Cl	Cl	B	47	12.0	26.6	16.7	16.7	16.9 ± 0.5	0.5 ± 1.6	
8e	Br	H	B	H-side	75	12.0	26.6	18.2	18.3	18.8 ± 0.3	1.8 ± 1.0
				Br-side	24	9.1	18.9	15.6	15.5	16.1 ± 0.3	2.2 ± 0.9
8g	Cl	Br	B	Cl-side	47	11.7	25.9	16.7			
				Br-side	47	10.8	23.9	16.7			
					45	15.2	28.3	16.4	16.6	17.1 ± 0.9	1.6 ± 2.8
9a			A	45	15.2	28.3	16.4	16.6	17.1 ± 0.9	1.6 ± 2.8	
9d			A	85	23.1	51.0	18.3	18.8	20.2 ± 1.0	4.8 ± 2.8	
9f			A	63	11.7	26.4	17.6	17.9	20.7 ± 1.0	9.4 ± 2.9	
12	C	A	A,A'-side	170	20.8	46.2	22.9				
			B,B'-side	110	35.8	79.6	19.3	19.1	18.7 ± 1.2	-1.3 ± 3.3	
			B,B'-side	115	15.4	34.2	20.2				

^a Solvent: A; CDCl₃, B; CD₂Cl₂, C; CD₂ClCD₂Cl.

**Figure 2.** Schematic potential energy diagram for the restricted rotation of pyrimidine ring in **8a-c** (A) and **8d-f** (B).

the Gutowsky–Holm approximation ($k_c = \pi\Delta\nu/\sqrt{2}$) and the ΔG_c^\ddagger value by using the Eyring equation, assuming a transmission coefficient of unity.¹² The ΔG_c^\ddagger values for **8a-c** were almost the same as each other (16.7 kcal/mol) within the experimental error. The energy barriers for the coalescence of the exchange were also calculated by a total line shape analysis. Thus, the calculation for **8a** afforded the kinetic parameters as $\Delta G_{298}^\ddagger = 16.6$ kcal/mol, $\Delta H^\ddagger = 15.9$ kcal/mol, and $\Delta S^\ddagger = -2.4$ eu at 25 °C. Tables 1 and S1 (supporting information) show the kinetic data for the other related 10-S-3 sulfuranes. There were observed two coalescence processes in monohalogenated 10-S-3 sulfuranes (**8d-f**), respectively. The coalescences at 21, 24, and 25 °C in **8d-f**, respectively, were assigned to the exchange process of the methyl groups in the 5-halogenated pyrimidine ring, and the other coalescences at 74, 75, and 70 °C were assigned to those in the nonhalogenated pyrimidine ring. The ΔG_c^\ddagger values for unsymmetrically dihalogenated molecules, **8g-i** were almost the same as each other within the experimental error.

The coalescence process can be explained by the restricted rotation of one of the pyrimidine rings in the 10-S-3 sulfuranes (**8a-i**) as illustrated in Figure 2. The energy maximum presumably refers to the conformation (transition state) where the two π -systems (pyrimidine ring and pyrimidinothiazole ring) are mutually perpendicular, generated by the cleavage of one side of the N–S–N hypervalent bond. The minimum corresponds to the planar conformation which is lower in energy resulting from the formation of the N–S–N hypervalent bond as well as the conjugation of the π -system (C=N=C=N). The symmetrical potential energy curve (A) of **8a-c** is understandable in terms of degenerate processes in which the left and right

Scheme 8

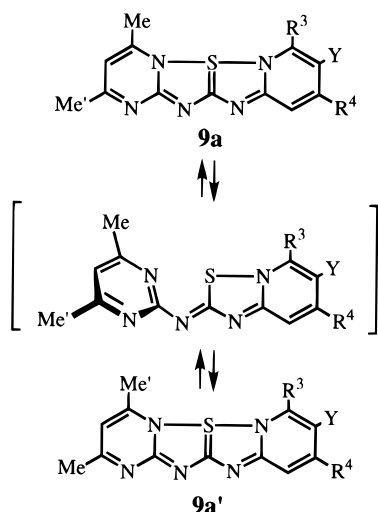
barriers are the same as each other ($\Delta G_{298}^\ddagger = 16.7$ kcal/mol). The restricted rotational energy barriers ($\Delta G_c^\ddagger = 16.7$ – 16.8 kcal/mol) of **8g-i** are almost the same as those ($\Delta G_c^\ddagger = 16.6$ – 16.8 kcal/mol) of **8a-c** in spite of different halogeno-substituents (X and Y) at both sides of the molecule. On the other hand, the rotational energy barriers (B) in **8d-f** are different for each side. It is noteworthy here that the activation free energy of the rotation of the halogenated pyrimidine ($\Delta G_{298}^\ddagger = 15.7$ kcal/mol) is lower than that ($\Delta G_{298}^\ddagger = 18.0$ kcal/mol) of the nonhalogenated pyrimidine in the unsymmetrical monohalogenated substrates (**8d-f**) at the same temperature.

The results can be attributed to the balance of the electron-withdrawing ability between both nitrogens in the hypervalent N–S–N bond. These can be visualized by difference of contribution of resonance canonical structures (Scheme 8). As the electron-withdrawing ability of halogenated ring increases relative to the other nonhalogenated one, the contribution of resonance structure (**8-i**; X = Cl, Br, I and Y = H) will increase relatively, and therefore the S–N bond is slightly elongated and attractive interaction in the halogenated pyrimidine side is weakened. In contrast, the S–N attractive interaction of the other side is strengthened. The imbalance of hypervalent bond (N–S–N) is qualitatively understandable in terms of the perturbational molecular orbital theory. When the unperturbed energy levels of the apical nitrogens become nondegenerate due to the difference of group electronegativity between both nitrogens, the bond strength between the less electronegative nitrogen moiety and the sulfur atom will increase relative to the other side.¹³ Notwithstanding, it is noticeable that the

(12) (a) Gutowsky, H. S.; Holm, C. H. *J. Chem. Phys.* **1956**, *25*, 1228. (b) Binsch, G. *Top. Stereochem.* **1968**, *3*, 97.

(13) Albright, T. A.; Burdett, J. K.; Whangbo, M.-H. *Orbital Interactions in Chemistry*; John Wiley & Sons, Inc.: New York, 1985; pp 36, 82.

Scheme 9



average of both rotational energy barriers (ΔG_c^\ddagger) is almost equal to that of the symmetrical system (**8a–c**).

Unsymmetric 10-S-3 Sulfurane. The two methyl peaks of the pyrimidine ring of **9a** coalesced at 45 °C, but the heteroaromatic peaks remained unchanged over the temperature range of spectral measurements. The exchange rate at the coalescence temperature was calculated by using the Gutowsky–Holm approximation to give $k_c = 28.3 \text{ s}^{-1}$.¹² Line shape analysis of the methyl group afforded the kinetic parameters as $\Delta G_{298}^\ddagger = 16.6 \text{ kcal/mol}$, $\Delta H^\ddagger = 17.1 \text{ kcal/mol}$, and $\Delta S^\ddagger = 1.6 \text{ eu}$ at 25 °C (see Table 1). The coalescence process can be also explained in terms of the rotation of the pyrimidine rings as shown in Scheme 9.

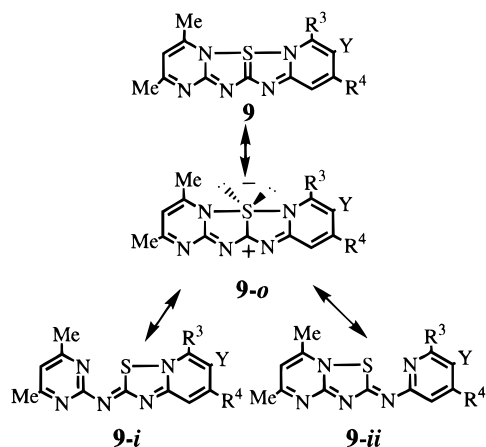
The rotation of the pyrimidine ring should afford two minima of potential due to two coordination sites of the pyrimidine ring, but the rotation of the pyridine ring must offer only single minimum potential in the internal rotation. The rotational energy barrier (ΔG_c^\ddagger : 16.6 kcal/mol) of the pyrimidine ring in **9a** was the same as that of **8a** (16.7 kcal/mol). The electronic effects of the fused pyridine ring influence the rotational energy barrier to almost the same degree as that of the fused pyrimidine ring in the present sulfurane. The similar temperature dependence in the ¹H NMR spectra were also observed in **9b–d**.

The rotation of the pyrimidine ring in **9d** is much slower than those in **9a–c** ($\Delta G_{298}^\ddagger = 16.1\text{--}16.6 \text{ kcal/mol}$), i.e., $k = 0.1 \text{ s}^{-1}$ and $\Delta G_{298}^\ddagger = 18.8 \text{ kcal/mol}$ at 25 °C. The chloro-substituent on the pyridine ring withdraws an electron to make the S–N(pyrimidine) bond stronger than those of **9a–c**, hence the rate is decelerated. This means that the contribution of resonance structure (**9-ii**; Y = Cl) in **9d** will increase relative to that (**9-ii**; Y = H) in **9a** (Scheme 10).

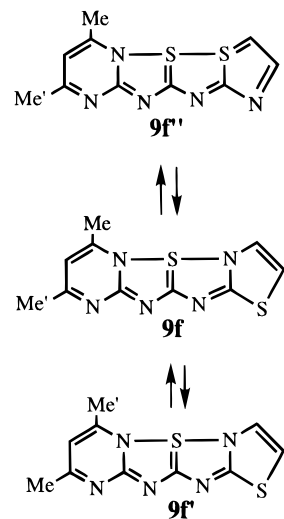
The analogous restricted rotation of pyrimidine ring was observed in 10-S-3 sulfurane (**9f**) fused with thiazole ring to give **9f'**. The rotational energy barrier (ΔG_c^\ddagger) was 17.6 kcal/mol. However, the rotation of the thiazole ring was not observed because the other isomer (**9f''**) produced by the rotation must be very unstable (Scheme 11). The degree of electronic effects of the thiazole ring to the rotational energy barrier seems to be almost the same order as that of the fused 3-chloropyridine ring in the present unsymmetric sulfurane **9**.

Furthermore, the ¹H NMR spectra of **24** as well as **18a,b** (Scheme 6, part a) did not change at all until –60 °C. The absence of temperature dependence in the ¹H NMR spectra suggests that the rotation of the pyrimidine ring of **18** and **24** about the C–N single bond suffered only small restriction until –60 °C (within NMR time scale). The rotational energy barrier can be calculated to be less than 11 kcal/mol by using the

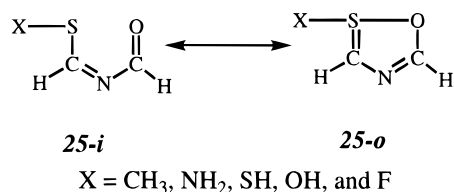
Scheme 10



Scheme 11



Scheme 12

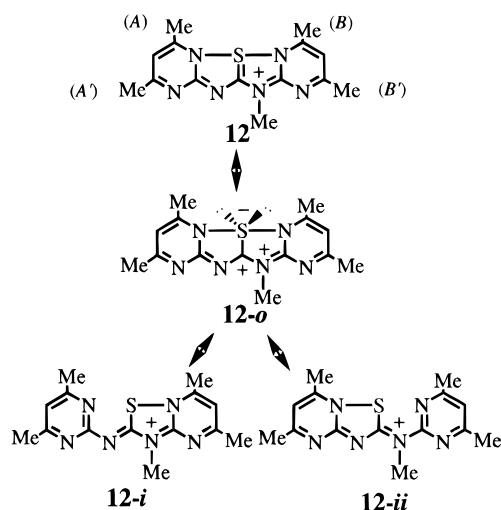


Gutowsky–Holm approximation based on the estimated difference of the chemical shifts of the two methyl groups ($\Delta\nu = 10 \text{ Hz}$; see Table 1).¹² Although the ring-transformation from **20a,b** to **21a,b** seems to occur *via* 10-S-3 sulfurane **20*a,b** as an intermediate and/or transition state, there was no evidence for such a hypervalent species at the ground state.

The sum of the energy stabilized by the N–S–N hypervalent bond and C=N–C=N π -conjugative stabilization in the present sulfurane system is evaluated on the basis of the kinetic data of the restricted rotation of the pyrimidine ring. The rotational energy barrier was estimated to be **less than** 11 kcal/mol which is mainly due to the π -conjugation in **18** and **24**. Therefore, the stabilization in **8a** by hypervalent N–S–N bond can be evaluated to be **at least** 6 kcal/mol. Csizmadia and his co-workers suggested that the energy of 1,5-S–O interaction in X–S–O hypervalent bond in a model system such as **25** in Scheme 12 is estimated as 6.58–15.45 kcal/mol by using 3-21G+ basis set.⁹

Monocationic 10-S-3 Sulfurane. Temperature dependence spectra were measured in the monocationic **12**. Two pairs of the methyl signals of **12**, i.e., CH₃(A)–CH₃(A') and CH₃(B)–CH₃(B')

Scheme 13



(B'), coalesced at 170 and 115 °C, respectively, and the ΔG_c^\ddagger values were calculated as 22.9 and 20.2 kcal/mol in CD_2Cl_2 (see Figure 1 and Table 1). Accordingly, the pyrimidine ring of the thiadiazolium side rotates more easily than the other pyrimidine ring in **12**. This difference of the rotational barrier is understandable in terms of the electronic effect to the rotation of the pyrimidine ring in the 10-S-3 sulfurane **12** according to the analogous considerations as described above in **8b–d** (Scheme 13). As the result of the stronger electron-withdrawing property of the thiadiazolium site as expected from the ^1H NMR data, the contribution of no-bond resonance structure **12-ii** should be increased, therefore, the S–N attractive interaction of this right side is weakened. The rotational barrier of **12** is larger than those of **8a–i**. The fact implies that a unit positive charge on **12** renders the hypervalent N–S–N bond stronger, probably and mainly due to electrostatic interaction between the sulfur and nitrogen atoms or decrease of the energy difference between the interacting orbitals of the sulfur and nitrogen atoms (*vide infra*).

Dicationic 10-S-3 Sulfurane. The coalescence of a pair of methyl signals at δ 2.83 and 2.99 in **17** was not observed until 132 °C in CD_3CN solution. Demethylation in **17** occurred gradually at 40 °C to give **12** without coalescence of the two methyl signals in $\text{DMSO}-d_6$. The rate constant of the demethylation to afford **12** was $4.5 \times 10^{-5} \text{ s}^{-1}$ at 80 °C. Therefore the rotational energy barrier was estimated to be greater than 21.2 kcal/mol according to the assumption of the coalescence temperature >132 °C of the methyl signals separated by 14.0 Hz at 90 MHz and the Gutowsky–Holm approximation.¹² This rotational energy barrier is higher than the other symmetric and unsymmetric sulfuranes described here.

Solvent Effects of the Restricted Rotation of the Pyrimidine Ring. The rotational energy barriers of **8a** and **12** in various solvents are shown in Table 2. The restricted rotational barrier in **8a** becomes higher in protic solvent such as $\text{CD}_3\text{OD}/\text{CDCl}_3$ or CF_3COOD than the pure CDCl_3 solution. The energy value (ΔG_c^\ddagger) in CF_3COOD was determined to be 19.6 kcal/mol at the coalescence temperature (100 °C) which was comparable to that (19.3 kcal/mol) of the cationic side (*B,B'*-side) of **12** in CDCl_3 . This shows that protonation to **8a** decelerates the rotation of the pyrimidine ring to almost the same degree as methylation at 12-position of **8a**. The solvent effect on the restricted rotation of pyrimidine ring in the monocationic 10-S-3 sulfurane (**12**) was investigated in several solvents. There was observed a linear relationship between the rotational energy barriers (ΔG_c^\ddagger) and the DN numbers as shown in Figure 3, but

Table 2. Solvent Effect on the Restricted Rotation in **8a** and **12**

compd/solvent	T_c (°C)	$\Delta\nu$ (Hz)	k_c (s^{-1})	ΔG_c^\ddagger (kcal/mol)
8a				
CDCl_3	44	12.5	27.8	16.6
$\text{CD}_3\text{OD}/\text{CDCl}_3$ (1:2)	54	15.2	33.7	16.9
CF_3COOD	100	11.2	24.9	19.6
12				
<i>A,A'</i> -side				
$\text{CD}_2\text{Cl}_2/\text{CD}_2\text{Cl}_2$	170	20.8	46.2	22.9
CD_3CN	146	15.3	34.0	21.9
$\text{DMSO}-d_6^a$	135	21.3	47.3	20.7
<i>B,B'</i> -side				
$\text{CD}_2\text{Cl}_2/\text{CD}_2\text{Cl}_2$	115	15.4	34.2	20.2
CDCl_3^a	110	35.8	79.6	19.3
$(\text{CD}_3)_2\text{CO}$	106	19.3	43.0	19.5
CD_3OD	94	13.7	30.4	19.1
CD_3CN	92	12.3	27.3	19.1
$\text{DMSO}-d_6^a$	89	14.5	32.2	18.8

^a Kinetic parameters: $\Delta G_{298}^\ddagger = 20.9$ kcal/mol, $\Delta H^\ddagger = 20.4 \pm 0.6$ kcal/mol, and $\Delta S^\ddagger = -0.5 \pm 1.5$ eu for *A,A'*-side of **12** in $\text{DMSO}-d_6$; $\Delta G_{298}^\ddagger = 19.1$ kcal/mol, $\Delta H^\ddagger = 18.7 \pm 1.2$ kcal/mol, and $\Delta S^\ddagger = -1.3 \pm 3.3$ eu for *B,B'*-side of **12** in CDCl_3 ; $\Delta G_{298}^\ddagger = 19.3$ kcal/mol, $\Delta H^\ddagger = 21.6 \pm 0.4$ kcal/mol, and $\Delta S^\ddagger = 7.6 \pm 1.2$ eu for *B,B'*-side of **12** in $\text{DMSO}-d_6$.

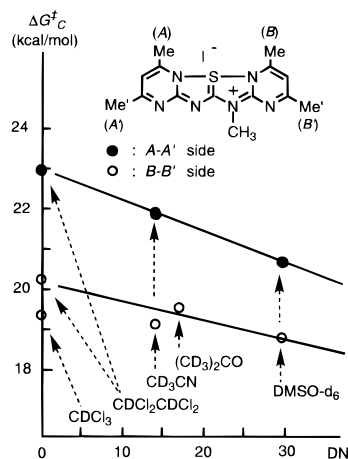


Figure 3. Solvent effect on the restricted rotation of pyrimidine ring in **12**.

there was no correlation between ΔG_c^\ddagger and the Dimroth–Reichardt's E_T values which are an approximate measure of Lewis acidity of solvents.^{14a,b} The larger the donor ability of the solvent is, the lower the barrier in rotation of the pyrimidine ring is. The Gutmann's donor number DN is expected to approximate to a measure of Lewis basicity of solvents.^{14c–f} The stabilization of transition state by nucleophilic solvation may contribute to lower the energy barrier in solvents with larger DN numbers. Therefore, it is considered that the nucleophilic solvation toward electron-deficient site of the molecule is more effective at the transition state (**12-tr-i** and **12-tr-ii**) than the ground state (planar form), because the positive charge delocalization is limited at the transition state (a half of molecular plane) relative to the ground state (a whole plane of molecule), as illustrated in Figure 4. It is not inconsistent with the present solvent effects that the energy maximum refers to the conforma-

(14) (a) Dimroth, K.; Reichardt, C.; Siepmann, T.; Bohlmann, F. *Justus Liebig's Ann. Chem.* **1963**, 661, 1. (b) Reichardt, C. *Solvent Effects in Organic Chemistry*, 2nd ed.; Verlag Chemie: Weinheim, 1988; p 365. (c) Gutmann, V.; Schmied, R. *Cood. Chem. Rev.* **1974**, 12, 263. (d) Gutmann, V. *Electrochim. Acta* **1976**, 21, 661. (e) Krygowsky, T. M.; Fawcett, W. R. *J. Am. Chem. Soc.* **1975**, 97, 2143. (f) Ohkata, K.; Nagai, T.; Tamaru, A.; Hanafusa, T. *J. Chem. Soc., Perkin Trans. 2* **1986**, 43.

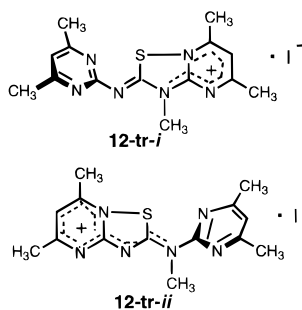


Figure 4. Transition state of the restricted rotation of pyrimidine ring in **12**.

tion where the two π systems are mutually perpendicular (pyrimidine ring and pyrimidinothiadiazole ring) as speculated above.

Isotope Exchange Study. Protons of the methyl group attached to heterocycles are more easily exchanged with deuterium than those of benzenoid aromatics under mild conditions in deuterated protic solvent such as MeOD.¹⁵ The activated methyl protons in pyridinium or pyrimidinium salts must exchange more smoothly than the corresponding neutral substrate. The reactivity should be dependent upon the relative position from the hetero atom. The ¹H NMR spectrum of monocationic **12** in CD₃OD showed four peaks at δ 2.75, 2.79, 2.90, and 3.00 for the methyl hydrogens of pyrimidine rings along with the other three signals at δ 4.18 for *N*-methyl hydrogens and at δ 7.39 and 7.47 for the pyrimidine ring hydrogens (Figure 1). Assignment of the methyl signals was achieved by comparisons of the ¹H NMR spectrum in **12** with that of a half deuterated derivative (**12-d₆**) prepared by the alternative synthesis as described above. It is noticeable that the methyl protons for CH₃(A) and CH₃(A') and H(a) protons appeared at lower magnetic field relative to those of the corresponding CH₃(B), CH₃(B'), and H(b) as shown in Figure 1.

The deuteration of the methyl groups attached to the pyrimidine ring of **12** was observed at 80 °C in CD₃OD solution by ¹H NMR spectroscopy. But the *N*-methyl hydrogens hardly undergo, if any, deuterium exchange reaction under the same conditions.

Rate determinations of the reaction in **12** and related compounds (**8a**, **9b**, and **18b**) were carried out ¹H NMR spectroscopically in CD₃OD solution at 80 °C under pseudo-first-order conditions. The rate constants were observed to drift slowly downward with proceeding of the reaction probably owing to the secondary deuterium isotope effect, and the values were also dependent on the concentration of the substrate. Accordingly, the kinetic study was carried out at the same concentration (1.36×10^{-2} mol/L) until one half-life. The rates were found to follow the first-order kinetics (correlation coefficients are more than 0.990). The rate constants are collected in Table 3. The deuterium exchange rates are very sensitive to the electronic properties of the heterocycle opposed to the dimethylpyrimidine ring.

The deuteration of a pair of the methyl groups (A and A' or B and B') in the same pyrimidine ring proceeded by the same rate constants. This phenomenon must result from the very much faster position-exchange (rotation: $k \sim 10^{-2}$ s⁻¹) of the methyl groups relative to the isotope exchange ($k = 10^{-5}$ – 10^{-4} s⁻¹).

Table 3. Reaction Rate Constants of Deuterium Exchange of the Methyl Hydrogens in **8a**, **9b**, **12**, and **18b**

compd	solvent ^a	$k_A, k_{A'} (s^{-1})$	$k_B, k_{B'} (s^{-1})$
8a	A	1.5×10^{-5}	
9b	B	1.7×10^{-6}	
12	A	2.4×10^{-5}	3.5×10^{-6}
12	B	4.3×10^{-4}	6.9×10^{-5}
18b	A	1.6×10^{-6}	
18b	B	1.5×10^{-6}	

^a Solvent: A; CD₃OD, B; CD₃OD/CDCl₃ (volume ratio is 1:1). Conditions: at 80 °C in 1.36×10^{-2} mol/L solution for each substance.

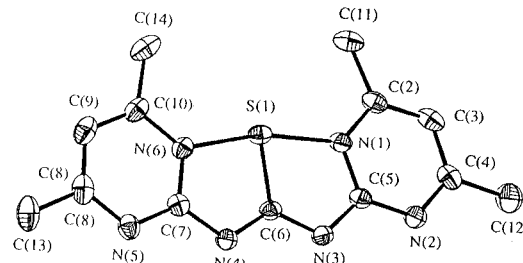


Figure 5. ORTEP drawing (30% probability ellipsoids) for **8a** (CH₂ClCH₂Cl)_{0.5}. Hydrogen atoms are omitted for clarity. Upper: a front view. Down: a ground plane.

It is noticeable that the methyl hydrogens (A and A') underwent the isotope exchange 6.2–6.8 times as fast as the methyl hydrogens (B and B') near the thiadiazolium part in **12**. The result indicates that the positive charge in **12** is more delocalized into the pyrimidine ring of the A,A'-side compared with the other pyrimidine ring of the B,B'-side which is closer to the thiadiazolium site. This is consistent with the chemical shift of the methyl group in the ¹H NMR spectrum (Figure 1). As expected, the isotope exchange reaction rate in the monocationic substrate (**12**) is 10 times faster than that of the neutral substrate (**8a**). The methyl hydrogens of the pyrimidine ring of **9b** underwent the isotope exchange 10 times more slowly than that of the neutral species (**8a**). It seems that the kinetic acidity in **9b** would decrease according to the increase of the electron density in the pyrimidine ring mainly through the N–S–N hypervalent bond due to the slight difference of electronegativity of the two heterocycles (pyrimidine > pyridine) according to the above considerations. It is also understandable that the reaction rate of the neutral system (**8a**) was 10 times faster than that of the benzothiazole system (**18b**) in which there is little or no N–S–C hypervalent bonding.

X-ray Structural Analysis of the 10-S-3 Sulfuranes 8a, 9a, and 17. Structures of **8a**, **17**, and **9a** are shown in Figures 5–7 as ORTEP drawings. Selected bond lengths and angles for these compounds are listed in Table 4.

The S–N bond distances (a_R and a_L) in **8a** are 1.948(3) and 1.934(3) Å. The corresponding bond distances (a_R and a_L) for **17** are 1.89(1) and 1.92(1) Å. These S–N distances are significantly longer than the sum of the sulfur and nitrogen

(15) (a) Dizabo, P.; Monier, J. C.; Pompon, A. J. *Label. Compounds* **1971**, 7, 399; *Chem. Abstr.* **1972**, 76, 85042g. (b) Balaban, A. T.; Gheorghiu, M. D.; Balaban, T. S. *J. Labelled Compd. Radiopharm.* **1983**, 20, 1097. (c) Balaban, A. T.; Balaban, T. S.; Uncuta, C.; Gheorghiu, M. D.; Chiraleu, F. J. *Labelled Compd. Radiopharm.* **1983**, 20, 1105.

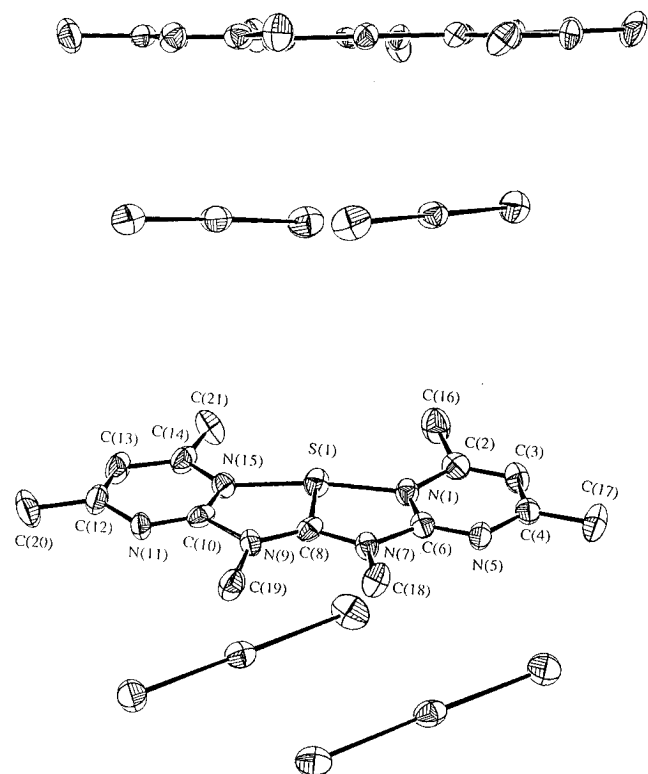


Figure 6. ORTEP drawing (30% probability ellipsoids) for **17**. Hydrogen atoms are omitted for clarity. Upper: a front view. Down: a ground plane.

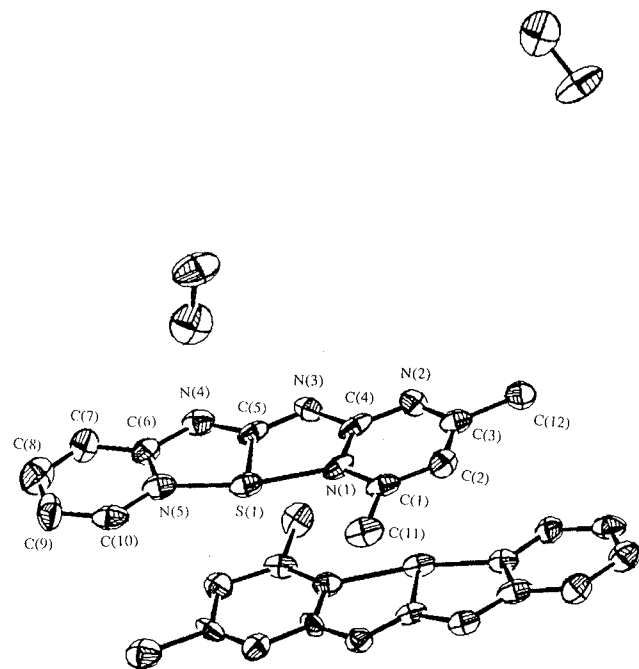


Figure 7. ORTEP drawing (30% probability ellipsoids) for **9-(CH₃OH)₂**. Hydrogen atoms are omitted for clarity.

covalent radii (1.70 Å).¹⁶ The S–N attractive interactions are estimated roughly to be 18.4 and 19.6 kcal/mol for **8a** and 20.9 and 24.0 kcal/mol for **17** by applying Huggins' equation.¹⁸ The distances are significantly shorter than the sum of the corresponding van der Waals radii (3.35 Å).¹⁷ The C–S–N bond angles [$\theta_R = 82.7(2)$, $\theta_L = 82.0(2)^\circ$] in **8a** are less than a right angle. The corresponding bond angles (θ_R and θ_L) in **17** are

Table 4. Selected Bond Lengths (Å) and Bond Angles (deg) for **8a**, **9a**, and **17**

structural parameter ^a		8a	9a	17
S–N	a_R	1.948(3)	2.01(1) (pyrim)	1.89(1)
S–N	a_L	1.934(3)	1.87(1) (py)	1.92(1)
S–C	b	1.787(4)	1.81(2)	1.76(1)
N–C	c_R	1.347(5)	1.32(2) (pyrim)	1.40(2)
N–C	c_L	1.337(5)	1.36(2) (py)	1.42(2)
N–S–C	θ_R	82.7(2)	80.5(6) (pyrim)	84.1(5)
N–S–C	θ_L	82.0(2)	84.5(6) (py)	83.0(5)

^a Bond length: a_R , a_L , b , c_R , and c_L (Å). Bond angle: θ_R and θ_L (deg).

84.1(5) and 83.0(5)°, respectively. The central sulfur atom (S) and the coordinated atoms (C, N, and N) in **8a** are virtually in the same molecular plane, respectively, as shown in Figure 5 (see the drawing at the top, a front view). The corresponding atoms (S, C, N, and N) in **17** are also in the same molecular plane as shown in Figure 6. These atoms in **17** form a plane [$-0.13277x + 0.9958y + 0.98613z = 5.54220$] with a mean deviation from the plane of 0.004 Å for the four atoms. All of these structural features are consistent with ψ -trigonal bipyramidal (ψ -TBP) geometry around the sulfur atom.

The apical positions are occupied by the two nitrogen atoms with N–S–N bond angle ($\theta_R + \theta_L$) for **8a** of 164.7(1)° and the corresponding bond angle for **17** of 167.1(5)°, respectively. In other words, the N–S–N bond angle in each case is bent away from a linear line toward the equatorial carbon atom. The distortion can be rationalized by considering the repulsive interaction between the sulfur lone pairs and bonding electrons of the apical ligand in **8a** and **17**, following the suggestion of Gillespie.¹⁹ A part of the deviation from ψ -TBP geometry may be attributed to the formation of the five-membered ring by including the long N–S bond.

The S–C bond length (b) in **8a** is 1.787(4) Å, which is essentially the same as the typical C–S single bond (1.78 Å for sp^2 -C–S) and very much longer than the typical C–S double bond (1.70 Å for C=S).¹⁶ The longer C–S bond length is understandable due to a considerable polarization of the C–S bond. The corresponding bond length (b) in **17** is 1.76(1) Å which is slightly shorter than a typical sp^2 -C–S single bond. The extra shortening of C–S bond in **17** would result from the presence of positive charges in the sulfurane.

Most of the C–N bond distances (1.330–1.37 Å) in the pyrimidino ring of **8a** and **17** are essentially the same, but the N–C bond distances (c_R and c_L) in **17** are slightly lengthened to 1.40(2) and 1.42(2) Å. The pivotal N–C bonds [$c_R = 1.347(5)$, $c_L = 1.337(5)$ Å] for the rotation of pyrimidine ring in **8a** are shorter than the typical sp^2 -C–N single bond length (1.43 Å) and approach to the typical sp^2 -C–N double bond length (1.30 Å).¹⁶ The values are close to that of acetamide (1.36 Å) or formamide (1.38 Å).¹⁶ On the other hand, the pivotal N–C bond lengths ($c_R = 1.40$ and $c_L = 1.42$ Å) in **17** are more close to the typical sp^2 -C–N single bond length (1.43 Å) rather than the typical double bond length (1.30 Å). The double bond character of the pivotal C–N bond in **8a** must influence the rotational energy barrier of the pyrimidine ring

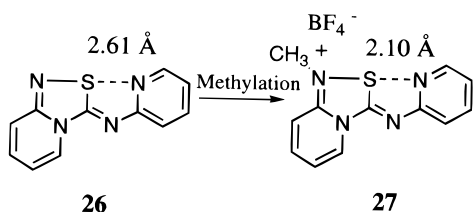
(16) Tables of Interatomic Distances and Configurations in Molecules and Ions; Sutton, L. E., Ed.; Special Publication No. 11, The Chemical Society: London, 1958; and Special Publication No. 18, 1965.

(17) Bondi, A. *J. Phys. Chem.* **1964**, *68*, 441.

(18) (a) Huggins, M. L. *J. Am. Chem. Soc.* **1953**, *75*, 4126. (b) Leung, F.; Nyburg, S. C. *Can. J. Chem.* **1972**, *50*, 324.

(19) (a) Gillespie, R. J. *J. Chem. Soc.* **1962**, *37*, 2498. (b) Gillespie, R. J. *Inorg. Chem.* **1966**, *5*, 1634. (c) Gillespie, R. J. *Can. J. Chem.* **1961**, *39*, 318. (d) Gillespie, R. J. *Can. J. Chem.* **1960**, *38*, 818.

Scheme 14



such as the restricted rotation of the amino group in amides.²⁰ It is justified to attribute an at least partial double bond character to the energy barrier of the restricted rotation of the pyrimidine ring. The restriction due to this factor should be larger in the neutral species (**8a**) than in the dicationic species (**17**). However, in fact, the rotational energy barrier in the dication **17** is significantly larger than that of neutral one (**8a**), i.e., >21 kcal/mol versus 17 kcal/mol. Since the pivotal C–N bond for the rotation of **17** is slightly longer than that of **8a**, the π -conjugation effect (double bond character) in the C–N bond can be ruled out in order to explain the increase of the rotational barrier height in **17** as compared with **8a**. Therefore, the increment of height in the rotational energy barrier does not arise mainly from such a double bond character of the C–N bond but from the other factor, for example, the increase of the N–S–N hypervalent bond strength of **17** resulted from the more positively charged sulfur atom than that of **8a**. By the same considerations the higher rotational energy barrier in the monocationic system (**12**) relative to **8a** may result from the more positively charged sulfuran. However, the influence of two counter ions (I_3^-) in **17** and one counter ion (I^-) in **12** might not be neglected in the case of evaluation of the rotational barrier, the contribution of which could not be measured experimentally.

In spite of unsymmetric character of the two fused heterocycles as shown in Figure 7, the structure of **9a** was almost similar to those of **8a** and **17**. All of the structural features are consistent with ψ -trigonal bipyramidal geometry. The S–N bond distances in **9a** are $a_R = 2.01(1)$ and $a_L = 1.87(1)$ Å. The S–N binding energy in **9a** are estimated to be 26.3 kcal/mol for the S–N(pyridine) and 13.8 kcal/mol for the S–N(pyrimidine) by the Huggins' equation.¹⁸ The most notable point in **9a** as compared with the structure data of **8a** and **17** is that the hypervalent bond is unsymmetrical. This result suggests that the electron-withdrawing property of the fused pyrimidine ring is larger than that of the fused pyridine ring which is quite consistent with the property of the two heterocycles.

Recently, L'abbe and his co-workers reported the structural features of unsymmetrical 10-S-3 sulfuranes (**26** and **27**) as shown in Scheme 14.¹⁰ They concluded on the basis of the X-ray structural data that there is little or no bonding between the sulfur atom and the pyridine nitrogen atom (2.61 Å) in the neutral system (**26**), but the methylated salt (**27**) has a closer S–N(pyridine) distance (2.10 Å) with an estimated bond dissociation energy of 6 kcal/mol.

Semiempirical MO Calculation of the 10-S-3 Sulfuran.

Semiempirical MO calculations by AM1 were performed on the two symmetric compounds **8a** and **17**. All geometrical parameters were obtained from the structural data from the X-ray analysis. The molecules were taken to lie in the x – y plane with S(1)–N(1) bond along the positive x axis as shown in Figure 8. The selected density matrixes, net atomic charges,

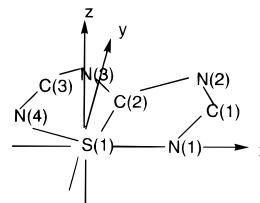


Figure 8. The orthogonal coordinates for MO calculation of **8a** and **17**.

Table 5. Selected Net Atomic Charges and Bond Orders in **8a** and **17**

position	net atomic charge		bond	bond order	
	8a	17		8a	17
S(1)	0.296	0.609	S(1)–N(1)	0.417	0.461
N(1)	–0.333	–0.333	S(1)–N(4)	0.439	0.402
N(2)	–0.190	–0.161	S(1)–C(2)	0.914	1.026
N(3)	–0.189	–0.125	C(1)–N(2)	1.239	0.988
N(4)	–0.335	–0.314	C(3)–N(3)	1.249	0.958
C(1)	0.184	0.209			
C(2)	0.085	0.131			
C(3)	0.187	0.175			

and bond orders were calculated by AM1 method, MOPAC Ver. 3.0.²¹ The selected density matrixes and coefficients for molecular orbitals around the sulfur atom in **8a** and **17** are shown in Tables S2 and S3, respectively. The selected net atomic charges and bond orders are shown in Table 5.

Several interesting points arise for these values. At first glance the electron distribution on the tetraazathiapentalene skeleton except for the sulfur atom remains almost unchanged between the neutral system (**8a**) and the dicationic system (**17**), in which the apical nitrogens become electron-rich site and the central sulfur atom is electron-deficient site as the typical hypervalent bond. In both cases the sulfur, carbon and hydrogen atoms carry substantial positive charges while net negative charges are concentrated on the nitrogens. The degree of electron deficiency at the sulfur atom in both systems is smaller than the formal charge of +1 which is literally expected from trivalent sulfonium sulfur atom. A significant amount of the positive charge (+2) on the dicationic 10-S-3 sulfurane generated by conversion from the neutral system (**8a**) to the dicationic system (**17**) distributes to the sulfur atom, in which the net charge increases from +0.3 to +0.6. The rest of the positive charges are partitioned on the electropositive 20 hydrogens, especially on the methyl groups (18 hydrogens: from 0.07–0.09 for **8a** to 0.12–0.13 for **17**). However, the electron density (net atomic charge derived from density matrix) at the apical nitrogen atoms remains almost unchanged in **8a** (–0.333, –0.335) and **17** (–0.333, –0.314). As expected from the X-ray structural data, the bond orders of the N–S bond in the dication **17** (0.402, 0.461) and the neutral **8a** (0.417, 0.439) are not different each other to any considerable extent.

The MOs and the energy levels of the hypervalent bond of **8a** and **17** (three-center four-electron bond) are illustrated in Figures 9 and 10, respectively. It is noticeable that a bonding character appears slightly between the sulfur atom (s-orbital) and the apical nitrogens (p_x -orbital) in nonbonding MO of the dicationic system (**17**) as shown in Figure 9 (cf. Table S3). Furthermore, Figure 10 shows that the level of bonding orbital

(20) (a) Lowe, J. P. *Prog. Phys. Org. Chem.*; Streitwieser, A., Jr., Taft, R. W., Eds.; John Wiley and Sons, Inc.: 1968; Vol. 6, p 1. (b) Kessler, H. *Angew. Chem., Int. Ed. Engl.* **1970**, *9*, 219. (c) Hammaker, R. W.; Gugler, B. A. *J. Mol. Spectrosc.* **1965**, *17*, 356. (d) Sunners, B.; Piette, L. H.; Schneider, W. G. *Can. J. Chem.* **1961**, *38*, 681. (e) Gutowsky, H. S.; Holm, C. H. *J. Chem. Phys.* **1956**, *25*, 1228.

(21) (a) Dewar, M. J. S.; Zoebisch, E. G.; Healy, E. F.; Stewart, J. J. P. *J. Am. Chem. Soc.* **1985**, *107*, 3902.

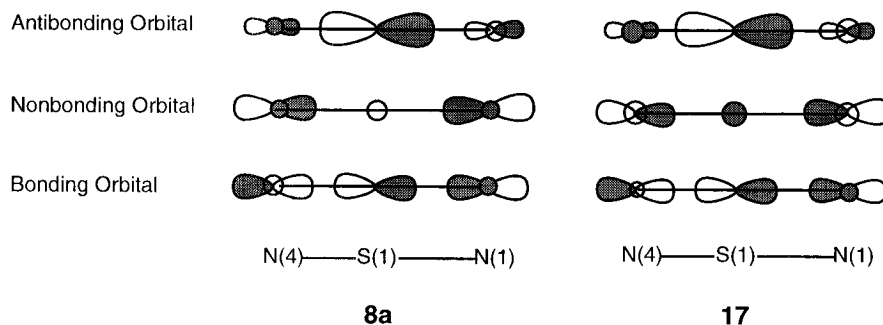


Figure 9. Schematic hypervalent bond in **8a** and **17**.

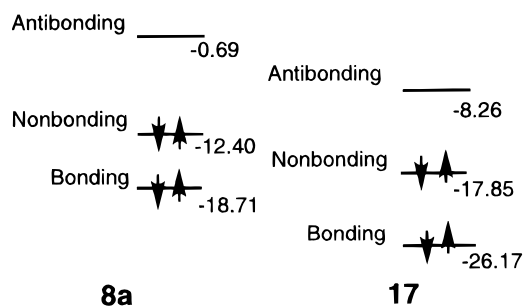


Figure 10. Energy level of the hypervalent bond of **8a** and **17** (eV).

in the dicationic system (**17**) is more lowered by a factor of 2.0 eV than that of the neutral system (**8a**) from each nonbonding level as a standard. This fact might contribute to strengthen the N–S–N hypervalent interaction along with electrostatic interaction in agreement with higher rotational barrier of pyrimidine ring in **17** than that of **8a**.

The π -type atomic overlapping between the sulfur and the equatorial carbon atom in **8a** is not so prominent relative to the σ -type overlapping (π -type: 0.2912 for $p_zS(1)-p_zC(2)$ vs σ -type: -0.7491 for $p_yS(1)-p_yC(2)$) as shown in Table S2 (supporting information). This fact suggests that the contribution of resonance canonical form bearing C–S double bond in **8** (see Scheme 8) is very small for stabilization of the present 10-S-3 sulfurane system. Furthermore, the π -type overlapping between the sulfur atom and the two apical nitrogen atoms which constitute the N–S–N hypervalent bond is also very small compared with the σ -type overlapping (0.1236 for $p_zS(1)-p_zN(1)$ vs -0.5386 for $p_xS(1)-p_xN(1)$). Therefore, it seems that the stabilization by delocalization of $(4n+2)\pi$ electrons in the planar five membered (thiadiazolo) rings does not contribute to the internal rotational energy barrier to significant extent.

Conclusions

The internal rotational energy barrier of the pyrimidine ring and N–S–N bond strength in 10-S-3 sulfuranes are highly sensitive to the balance of the electron-withdrawing ability between both nitrogens in the hypervalent N–S–N bond. When a qualitative valence bond language is used, the phenomena can be visualized by the different degree of contribution of resonance structures.

According to structural considerations by both X-ray analysis and semiempirical MO calculation, the symmetric resonance canonical form should be depicted with a polarized form as shown in **8-o**. The internal rotational energy barrier is more than 4 kcal/mol higher in the dicationic system (**17**) than the neutral system (**8a**). This can be attributed mainly to the increase of the strength of the N–S–N hypervalent bond.

Experimental Section

All the melting points are uncorrected. IR spectra were obtained with a Shimadzu IR-460 grating IR spectrophotometer. 1H NMR

measurements were carried out on Hitachi R-90H and JEOL EX-400 instruments, using tetramethylsilane as the internal reference. Temperatures in the probe were calibrated using the chemical shift difference of ethylene glycol.

General Procedure for Preparation of the Isothiocyanates 6a–c. To a mixture of 2-amino-4,6-dimethylpyrimidine (**5a**, 1.5 g, 12 mmol) and sodium hydrogen carbonate (2.5 g, 30 mmol) in dichloromethane (50 mL) was added a solution of thiophosgene (0.91 mL, 12 mmol) with vigorous stirring. After the mixture was heated at reflux temperature for 6 h, the mixture was poured into water, and the product was extracted into dichloromethane before drying over $MgSO_4$. The organic solution was concentrated and column chromatographic separation on silica gel (*n*-hexane–ethyl acetate; 1:1) gave 2-(4,6-dimethylpyrimidinyl)isothiocyanate **6a** (1.5 g) as an oily product in 74% yield. The isothiocyanate **6a** was used for the following reaction without further purification. By the same procedure **6b** (60%) and **6c** (26%) were prepared. For **6a**: 1H NMR ($CDCl_3$) δ 2.46 (s, 6H), 6.91 (s, 1H); IR (neat) ν_{max} 2005, 1999, 1589, 1531, 1430, 1338 cm^{-1} . For **6b**: 1H NMR ($CDCl_3$) δ 2.57 (s, 6H); IR (KBr) ν_{max} 2005, 1999, 1558, 1556, 1352, 1332 cm^{-1} . For **6c**: 1H NMR ($CDCl_3$) δ 2.61 (s, 6H); IR (KBr) ν_{max} 2080, 2015, 1995, 1551, 1549, 1547, 1543, 1517, 1416, 1346 cm^{-1} .

General Procedure for Preparation of the S-Methyl Dithiocarbamates 6f–j. A mixture of 2-aminopyridine (**5f**, 19.0 g, 0.20 mol), carbon disulfide (12 mL, 0.19 mol), and triethylamine (30 mL, 0.21 mol) was heated at reflux temperature for 2 h. The mixture was filtered and the resultant solid was washed with ether to give triethylammonium dithiocarbamate (40.9 g). To the crude dithiocarbamate (13.6 g) in dichloromethane (50 mL) was added methyl iodide (3.11 mL, 50 mmol) at 0 °C. After stirring of the solution for 12 h, the mixture was poured into water and the product was extracted into dichloromethane. After flash-column chromatographic separation on silica gel (*n*-hexane:ethyl acetate = 4:1), 8.20 g of **6f** was obtained.

S-Methyl 2-pyridinyldithiocarbamate (6f): 68% yield based on **5f**; mp 90 °C (lit.²² 91 °C); 1H NMR ($CDCl_3$) δ 2.68 (s, 3H), 7.10 (dd, $J = 6.2, 2.4$ Hz, 1H), 7.75 (dd, $J = 8.4, 6.2$ Hz, 1H), 8.2–8.7 (m, 2H), 10.6 (bs, 1H).

S-Methyl 4-methyl-2-pyridinyldithiocarbamate (6g): 66% yield based on **5g**; mp 99–100 °C (lit.²² 101–102 °C).

S-Methyl 6-methyl-2-pyridinyldithiocarbamate (6h): 58% yield based on **5h**; mp 89–90 °C (lit.²² 89–90 °C).

S-Methyl 5-chloro-2-pyridinyldithiocarbamate (6i): 3% yield based on **5i**; 157 °C; 1H NMR ($CDCl_3$) δ 2.68 (s, 3H), 7.69 (dd, $J = 9.0, 2.4$ Hz, 1H), 8.34 (d, $J = 2.4$ Hz, 1H), 8.60 (d, $J = 9.0$ Hz, 1H), 9.64 (bs, 1H).

S-Methyl 2-thiazolyldithiocarbamate (6j): 25% yield based on **5j**; mp 179–181 °C; 1H NMR ($CDCl_3$) δ 2.72 (s, 3H), 6.94 (d, $J = 3.8$ Hz, 1H), 7.75 (d, $J = 3.8$ Hz, 1H).

General Procedure for Preparation of the Thioureas 7a–c. To a mixture of 2-amino-4,6-dimethylpyrimidine (**5a**, 7.37 g, 59.8 mmol) and sodium hydrogen carbonate (5.92 g, 70.5 mmol) in 100 mL of acetonitrile was added thiophosgene (2.4 mL, 31 mmol), and the mixture was heated at reflux temperature for 22 h. The mixture was poured into water and the resultant precipitates were separated by filtration. Recrystallization of the precipitates from *n*-hexane–dichloromethane gave **7a** as a pure sample.

N,N'-Bis(4,6-dimethyl-2-pyrimidinyl)thiourea (**7a**): 90% yield; mp 231–232 °C; ¹H NMR (CDCl₃) δ 2.48 (s, 12H) 6.79 (s, 2H), 7.4–9.0 (bs, 1H), 13.0–14.0 (bs, 1H); IR (KBr) ν_{\max} 1606, 1515, 1421, 1365, 1348, 1337, 1301, 1189, 1164 cm⁻¹.

N,N'-Bis(5-chloro-4,6-dimethyl-2-pyrimidinyl)thiourea (**7b**): 92% yield; mp 228–229 °C (methanol); ¹H NMR (CDCl₃) δ 2.60 (s, 12H), 7.5–9.0 (bs, 1H), 13.0–14.0 (bs, 1H).

N,N'-Bis(5-bromo-4,6-dimethyl-2-pyrimidinyl)thiourea (**7c**): 63% yield; mp 242–244 °C (methanol); ¹H NMR (CDCl₃) δ 2.64 (s, 12H), 8.0–9.0 (bs, 1H), 13.0–14.0 (bs, 1H).

General Procedure for Preparation of the Thioureas 7d–i. A mixture of 2-amino-5-chloro-4,6-dimethylpyrimidine **5b** (366.9 mg, 2.33 mmol) and 2-(4,6-dimethylpyrimidinyl)isothiocyanate (**6a**) in 15 mL of acetonitrile was heated at reflux temperature for 20 h. The mixture was filtered, and the solid was recrystallized from methanol to give a pure sample **7d** (550 mg).

N-(5-Chloro-4,6-dimethyl-2-pyrimidinyl)-*N'*-(4,6-dimethyl-2-pyrimidinyl)thiourea (**7d**): 79% yield; mp 209–211 °C (methanol); ¹H NMR (CDCl₃) δ 2.47 (s, 6H), 2.60 (s, 6H), 6.77 (s, 1H), 8.0–9.0 (bs, 1H), 13.0–14.0 (bs, 1H); IR (KBr) ν_{\max} 1602, 1538, 1426, 1384, 1343, 1308, 1174 cm⁻¹.

N-(5-Bromo-4,6-dimethyl-2-pyrimidinyl)-*N'*-(4,6-dimethyl-2-pyrimidinyl)thiourea (**7e**): 45% yield from **6a** and **5c**; mp 235–236 °C (methanol); ¹H NMR (CDCl₃) δ 2.47 (s, 6H), 2.65 (s, 6H), 6.77 (s, 1H), 8.0–9.0 (bs, 1H), 13.0–14.0 (bs, 1H).

N-(5-Iodo-4,6-dimethyl-2-pyrimidinyl)-*N'*-(4,6-dimethyl-2-pyrimidinyl)thiourea (**7f**): 78% yield from **6a** and **5d**; mp 252–253 °C (methanol); ¹H NMR (CDCl₃) δ 2.48 (s, 6H), 2.72 (s, 6H), 6.78 (s, 1H), 8.0–9.0 (bs, 1H), 13.0–14.0 (bs, 1H).

N-(5-Bromo-4,6-dimethyl-2-pyrimidinyl)-*N'*-(5-chloro-4,6-dimethyl-2-pyrimidinyl)thiourea (**7g**): 94% yield from **6b** and **5c**; mp 233–234 °C (methanol); ¹H NMR (CDCl₃) δ 2.60 (s, 6H), 2.64 (s, 6H), 8.0–9.2 (bs, 1H), 13.0–14.0 (bs, 1H).

N-(5-Chloro-4,6-dimethyl-2-pyrimidinyl)-*N'*-(5-iodo-4,6-dimethyl-2-pyrimidinyl)thiourea (**7h**): 99% yield from **6b** and **5d**; mp 242–243 °C (dichloromethane); ¹H NMR (CDCl₃) δ 2.60 (s, 6H), 2.72 (s, 6H), 8.0–9.0 (bs, 1H), 13.0–14.0 (bs, 1H).

N-(5-Bromo-4,6-dimethyl-2-pyrimidinyl)-*N'*-(5-iodo-4,6-dimethyl-2-pyrimidinyl)thiourea (**7i**): 100% yield from **6c** and **5d**; mp 234–236 °C (dichloromethane); ¹H NMR (CDCl₃) δ 2.64 (s, 6H), 2.72 (s, 6H), 8.0–9.0 (bs, 1H), 13.0–14.0 (bs, 1H).

General Procedure for Preparation of the Thioureas 7j–p. A mixture of 2-amino-4,6-dimethylpyrimidine (**5a**) (2.46 g, 20 mmol) and *S*-methyl 2-pyridinylthiocarbamate **6f** (3.68 g, 20 mmol) in 50 mL toluene was heated at reflux temperature. The resultant solid was recrystallized from methanol to give **7j** (3.4 g).

N-(4,6-Dimethyl-2-pyrimidinyl)-*N'*-2-pyridinylthiourea (**7j**): 66% yield; mp 191–193 °C; ¹H NMR (CDCl₃) δ 2.49 (s, 6H), 6.74 (s, 1H), 7.10 (dd, *J* = 6.4, 5.1 Hz, 1H), 7.74 (dd, *J* = 8.4, 6.4 Hz, 1H), 8.39 (d, *J* = 5.1 Hz, 1H), 8.6 (bs, 1H), 8.90 (d, *J* = 8.4 Hz, 1H), 13.8 (bs, 1H).

N-(4,6-Dimethyl-2-pyrimidinyl)-*N'*-(6-methyl-2-pyridinyl)thiourea (**7k**): 59% yield from **5a** and **6h**; mp 178 °C (methanol); ¹H NMR (CDCl₃) δ 2.48 (s, 6H), 2.51 (s, 3H), 6.73 (s, 1H), 6.97 (d, *J* = 7.9 Hz, 1H), 7.63 (t, *J* = 7.9 Hz, 1H), 8.57 (bs, 1H), 8.65 (d, *J* = 7.9 Hz, 1H), 13.7 (bs, 1H).

N-(4,6-Dimethyl-2-pyrimidinyl)-*N'*-(4-methyl-2-pyridinyl)thiourea (**7l**): 55% yield from **5a** and **6g**; mp 184 °C (methanol); ¹H NMR (CDCl₃) δ 2.41 (s, 3H), 2.48 (s, 6H), 6.72 (s, 1H), 6.92 (d, *J* = 5.3 Hz, 1H), 8.24 (d, *J* = 5.3 Hz, 1H), 8.6 (bs, 1H), 8.72 (s, 1H), 13.8 (bs, 1H).

N-(4,6-Dimethyl-2-pyrimidinyl)-*N'*-(5-chloro-2-pyridinyl)thiourea (**7m**): 85% yield from **5a** and **6i**; mp 242 °C (methanol); ¹H NMR (CDCl₃) δ 2.48 (s, 6H), 6.75 (s, 1H), 7.70 (dd, *J* = 9.0, 2.6 Hz, 1H), 8.33 (d, *J* = 2.6 Hz, 1H), 8.6 (bs, 1H), 8.96 (d, *J* = 9.0 Hz, 1H), 14.0 (bs, 1H).

N-(4-Methyl-2-pyrimidinyl)-*N'*-2-pyridinylthiourea (**7n**): 69% yield from **5e** and **6f**; mp 213–214 °C (methanol); ¹H NMR (CDCl₃) δ 2.54 (s, 3H), 6.88 (d, *J* = 5.1 Hz, 1H), 7.11 (dd, *J* = 6.2, 5.1 Hz, 1H), 7.75 (dd, *J* = 8.6, 6.2 Hz, 1H), 8.41 (d, *J* = 5.1 Hz, 1H), 8.50 (d, *J* = 5.1 Hz, 1H), 8.8 (bs, 1H), 8.92 (d, *J* = 8.6 Hz, 1H), 13.7 (bs, 1H).

N-(4,6-Dimethyl-2-pyrimidinyl)-*N'*-2-thiazolylthiourea (**7o**): 65% yield from **5a** and **6j**; mp 233–234 °C (methanol); ¹H NMR (CDCl₃)

δ 2.51 (s, 6H), 6.77 (s, 1H), 6.98 (d, *J* = 3.6 Hz, 1H), 7.57 (d, *J* = 3.6 Hz, 1H), 8.6 (bs, 1H), 15.0 (bs, 1H).

N,N'-Bis(4-methyl-2-pyridinyl)thiourea (**7p**): 86% yield from **5g** and **6g**; mp 190–192 °C (methanol); ¹H NMR (CDCl₃) δ 2.38 (s, 6H), 6.89 (d, *J* = 5.3 Hz, 2H), 8.24 (d, *J* = 5.3 Hz, 2H), 6.5–8.5 (m, 2H).

2,4,8,10-Tetramethyl-6*l*⁴-pyrimido[1'',2'':2',3'][1,2,4]thiadiazolo[1',5':1,5][1,2,4]-thiadiazolo[2,3-*a*]pyrimidine (**8a**). A mixture of 1.514 g (6.2 mmol) of **7a** and sulfuryl chloride (0.42 mL) in dichloromethane (100 mL) was stirred at room temperature for 1 day. To the reaction mixture was added ca. 2 g of sodium hydrogen carbonate, and the mixture was stirred overnight at room temperature. The resultant mixture was filtered, and the filtrate was dried over MgSO₄. After solvent removal, the resultant solid was recrystallized from dichloromethane to give a pure sample **8a** in 86% yield: mp > 300 °C; ¹H NMR (CDCl₃) δ 2.56 (s, 6H), 2.67 (s, 6H), 6.57 (s, 2H); ¹³C NMR (CDCl₃) δ 19.69, 24.90, 111.38, 155.77, 160.76, 171.31. The thiocarbonyl (C=S) peak was not observed: IR (KBr) ν_{\max} 1592, 1491, 1449, 1425, 1338 cm⁻¹; UV (CHCl₃) λ_{\max} nm (ϵ) 340 (26 000), 302 (15 000), 250 (18 000).

General Procedure for Preparation of the 10-S-3 Sulfuranes 8b–e and 8g by Oxidation with NBS. A mixture of 123.3 mg (0.35 mmol) of **7b** and *N*-bromosuccinimide (62.9 mg, 0.35 mmol) in dichloromethane (30 mL) was stirred at room temperature for 2 h. To the mixture was added 20 mL of water, and the product was extracted into dichloromethane. After the organic layer was dried over MgSO₄, solvent removal afforded the solid product. Recrystallization of the solid from dichloromethane gave 123 mg of **8b** as a pure sample.

3,9-Dichloro-2,4,8,10-tetramethyl-6*l*⁴-pyrimido[1'',2'':2',3'][1,2,4]-thiadiazolo[1',5':1,5][1,2,4]-thiadiazolo[2,3-*a*]pyrimidine (**8b**): 99% yield; mp > 300 °C (dichloromethane); ¹H NMR (CDCl₃) δ 2.69 (s, 6H), 2.83 (s, 6H); IR (KBr) ν_{\max} 1521, 1490, 1439, 1364, 1319 cm⁻¹.

3,9-Dibromo-2,4,8,10-tetramethyl-6*l*⁴-pyrimido[1'',2'':2',3'][1,2,4]-thiadiazolo[1',5':1,5][1,2,4]-thiadiazolo[2,3-*a*]pyrimidine (**8c**): 98% yield; mp > 300 °C (dichloromethane); ¹H NMR (CDCl₃) δ 2.72 (s, 6H), 2.84 (s, 6H).

3-Chloro-2,4,8,10-tetramethyl-6*l*⁴-pyrimido[1'',2'':2',3'][1,2,4]-thiadiazolo[1',5':1,5][1,2,4]-thiadiazolo[2,3-*a*]pyrimidine (**8d**): 84% yield; mp > 300 °C (dichloromethane); ¹H NMR (CDCl₃) δ 2.58 (s, 3H), 2.72 (bs, 3H), 2.73 (s, 6H), 6.65 (q, *J* = 0.44 Hz, 1H).

3-Bromo-2,4,8,10-tetramethyl-6*l*⁴-pyrimido[1'',2'':2',3'][1,2,4]-thiadiazolo[1',5':1,5][1,2,4]-thiadiazolo[2,3-*a*]pyrimidine (**8e**): 77% yield; mp > 300 °C (dichloromethane); ¹H NMR (CDCl₃) δ 2.57 (s, 3H), 2.72 (d, *J* = 0.66 Hz, 3H), 2.75 (s, 6H), 6.62 (q, *J* = 0.66 Hz, 1H).

3-Bromo-9-chloro-2,4,8,10-tetramethyl-6*l*⁴-pyrimido[1'',2'':2',3'][1,2,4]thiadiazolo[1',5':1,5][1,2,4]-thiadiazolo[2,3-*a*]pyrimidine (**8g**): 77% yield; mp > 300 °C (dichloromethane); ¹H NMR (CDCl₃) δ 2.68 (s, 3H), 2.72 (s, 3H), 2.81 (s, 3H), 2.84 (s, 3H).

General Procedure for Preparation of 8f,h,i by Oxidation with NCS. A mixture of **7f** (111.9 mg, 0.2 mmol) and *N*-chlorosuccinimide (37.4 mg, 0.28 mmol) in dichloromethane (30 mL) was stirred for 7 h at room temperature. To the mixture was added 20 mL of water, and the precipitates were obtained by filtration. The resultant solid product was recrystallized from dichloromethane to afford 38.9 mg of **8f** as a pure sample.

3,9-Iodo-2,4,8,10-tetramethyl-6*l*⁴-pyrimido[1'',2'':2',3'][1,2,4]thiadiazolo[1',5':1,5][1,2,4]-thiadiazolo[2,3-*a*]pyrimidine (**8f**): 47% yield; mp 270 °C dec; ¹H NMR (CDCl₃) δ 2.58 (s, 3H), 2.72 (d, *J* = 0.66 Hz, 3H), 2.84 (bs, 6H), 6.65 (q, *J* = 0.66 Hz, 1H); IR (KBr) ν_{\max} 1601, 1536, 1509, 1477, 1415, 1363, 1347, 1320, 786 cm⁻¹.

3-Chloro-9-iodo-2,4,8,10-tetramethyl-6*l*⁴-pyrimido[1'',2'':2',3'][1,2,4]thiadiazolo[1',5':1,5][1,2,4]-thiadiazolo[2,3-*a*]pyrimidine (**8h**): 40% yield; mp > 300 °C (dichloromethane); ¹H NMR (CDCl₃) δ 2.72 (s, 3H), 2.83 (s, 6H), 2.94 (s, 3H).

3-Bromo-9-iodo-2,4,8,10-tetramethyl-6*l*⁴-pyrimido[1'',2'':2',3'][1,2,4]thiadiazolo[1',5':1,5][1,2,4]-thiadiazolo[2,3-*a*]pyrimidine (**8i**): 35% yield; mp > 300 °C (dichloromethane); ¹H NMR (CDCl₃) δ 2.75 (s, 3H), 2.84 (s, 6H), 2.95 (s, 3H).

General Procedure for Preparation of the 10-S-3 Sulfurane 9a–f and 10 by Oxidation with SO₂Cl₂. A mixture of 260 mg (1 mmol) of **7j** and sulfuryl chloride (0.1 mL, 1.2 mmol) in dichloromethane (20 mL) was stirred at room temperature for 1 day. To the reaction mixture was added ca. 1 g of sodium hydrogen carbonate, and the mixture was

stirred overnight at room temperature. The resultant mixture was filtered, and the filtrate was dried over MgSO₄. After solvent removal, the resultant solid was recrystallized from acetone to give 220 mg of **9a** as a pure sample.

2,4-Dimethyl-6 λ^4 -pyrido[1'',2'':2',3'][1,2,4]-thiadiazolo[1',5':1,5]-[1,2,4]thiadiazolo[2,3-*a*]pyrimidine (**9a**): 86% yield; mp 234–235 °C (acetone); ¹H NMR (CDCl₃) δ 2.54 (s, 3H), 2.68 (s, 3H), 6.54 (s, 1H), 6.89 (ddd, *J* = 8.1, 6.2, 1.8 Hz, 1H), 7.53 (dd, *J* = 8.6, 1.8 Hz, 1H), 7.63 (ddd, *J* = 8.6, 8.1, 1.5 Hz, 1H), 8.31 (dd, *J* = 6.2, 1.5 Hz, 1H).

2,4,8-Trimethyl-6 λ^4 -pyrido[1'',2'':2',3'][1,2,4]-thiadiazolo[1',5':1,5]-[1,2,4]thiadiazolo[2,3-*a*]pyrimidine (**9b**): 55% yield; mp 265 °C (acetone); ¹H NMR (CDCl₃) δ 2.4–2.8 (bs, 6H), 2.74 (s, 3H), 6.53 (s, 1H), 6.69 (d, *J* = 6.6 Hz, 1H), 7.44 (d, *J* = 8.6 Hz, 1H), 7.62 (dd, *J* = 8.6, 6.6 Hz, 1H).

2,4,10-Trimethyl-6 λ^4 -pyrido[1'',2'':2',3'][1,2,4]-thiadiazolo[1',5':1,5][1,2,4]thiadiazolo[2,3-*a*]pyrimidine (**9c**): 83% yield; mp 235–236 °C (acetone); ¹H NMR (CDCl₃) δ 2.41 (s, 3H), 2.52 (s, 3H), 2.65 (s, 3H), 6.51 (s, 1H), 6.71 (d, *J* = 6.2 Hz, 1H), 7.31 (s, 1H), 8.14 (d, *J* = 6.2 Hz, 1H).

9-Chloro-2,4-dimethyl-6 λ^4 -pyrido[1'',2'':2',3'][1,2,4]-thiadiazolo[1',5':1,5][1,2,4]thiadiazolo[2,3-*a*]pyrimidine (**9d**): 69% yield; mp > 300 °C (acetone); ¹H NMR (CDCl₃) δ 2.57 (s, 3H), 2.71 (s, 3H), 6.59 (s, 1H), 7.49 (d, *J* = 9.1 Hz, 1H), 7.66 (dd, *J* = 9.1, 2.2 Hz, 1H), 8.35 (d, *J* = 2.2 Hz, 1H).

2(or 4)-Methyl-6 λ^4 -pyrido[1'',2'':2',3'][1,2,4]-thiadiazolo[1',5':1,5]-[1,2,4]thiadiazolo[2,3-*a*]pyrimidine (**9e** or **9e'**): 90% yield; mp 246 °C (acetone); ¹H NMR (CDCl₃) δ 2.6–2.8 (3H), 6.5–6.8 (1H), 6.94 (dt, *J* = 6.4, 1.8 Hz, 1H), 7.58 (d, *J* = 8.6 Hz, 1H), 7.73 (ddd, *J* = 8.6, 6.4, 1.5 Hz, 1H), 8.29 (d, *J* = 6.4 Hz, 1H), 8.3–8.7 (1H), at 10 °C δ [2.62 (s), 2.77 (s), 3H], [6.69 (d, *J* = 4.8 Hz) 6.77 (d, *J* = 4.8 Hz), 1H], 6.96 (dt, *J* = 6.4, 1.5 Hz, 1H), 7.58 (d, *J* = 8.8 Hz, 1H), 7.70 (ddd, *J* = 8.8, 6.4, 1.5 Hz, 1H), 8.36 (d, 6.4 Hz, 1H), [8.43 (d, *J* = 4.8 Hz), 8.69 (d, *J* = 4.8 Hz)].

2,4-Dimethyl-6 λ^4 -thiadiazolo[3'',2'':2',3'][1,2,4]-thiadiazolo[1',5':1,5][1,2,4]thiadiazolo[2,3-*a*]pyrimidine (**9f**): 76% yield; mp 235–238 °C (acetone); ¹H NMR (CDCl₃) δ 2.58 (s, 3H), 2.70 (s, 3H), 6.61 (s, 1H), 6.85 (d, *J* = 4.0 Hz, 1H), 7.51 (d, *J* = 4.0 Hz, 1H).

2,10-Dimethyl-6 λ^4 -pyrido[1'',2'':2',3'][1,2,4]-thiadiazolo[1',5':1,5]-[1,2,4]thiadiazolo[2,3-*a*]pyridine (**10**): 90% yield; mp 240–241 °C (CH₂Cl₂–acetone); ¹H NMR (CDCl₃) δ 2.39 (s, 6H), 6.69 (dd, *J* = 6.2, 1.3 Hz, 2H), 7.24 (d, *J* = 1.3 Hz, 2H), 8.13 (d, *J* = 6.2 Hz, 2H); ¹³C NMR (CDCl₃) δ 21.39, 115.47, 117.68, 132.88, 148.76, 156.02, 168.01.

General Procedure for Alkylation of the 10-S-3 Sulfurane 8a, 8d, 9a, and 10. To a solution of **8a** (112.2 mg, 0.39 mmol) in dichloromethane (20 mL) was added methyl iodide (223.5 mg, 1.57 mmol), and the mixture was heated at reflux temperature for 13 h. Concentration of the mixture afforded a solid product. Recrystallization of the solid from dichloromethane–*n*-hexane gave a pure sample of **12**.

2,4,8,10,12-Pentamethyl-6 λ^4 -pyrimido[1'',2'':2',3'][1,2,4]thiadiazolo[1',5':1,5][1,2,4]thiadiazolo[2,3-*a*]pyrimidinium iodide (**12**): 78% yield; mp 242–245 °C dec; ¹H NMR (CDCl₃) δ 2.65 (s, 3H), 2.73 (s, 3H), 3.03 (d, *J* = 0.65 Hz, 3H), 3.23 (d, *J* = 0.66 Hz, 3H), 4.11 (s, 3H), 7.16 (q, *J* = 0.65 Hz, 1H), 7.30 (q, *J* = 0.66 Hz, 1H); ¹³C NMR (acetone-*d*₆) δ 20.42, 20.53, 25.27, 25.67, 33.96, 117.44, 118.17, 153.85, 157.73, 159.82, 163.97, 167.28, 174.85, 176.15.

3-Chloro-2,4,8,10,12-pentamethyl-6 λ^4 -pyrimido[1'',2'':2',3'][1,2,4]-thiadiazolo[1',5':1,5][1,2,4]thiadiazolo[2,3-*a*]pyrimidinium iodide (**13-F**) and **3-chloro-2,4,8,10,13-pentamethyl-6 λ^4 -pyrimido[1'',2'':2',3']**[1,2,4]-thiadiazolo[1',5':1,5][1,2,4]thiadiazolo[2,3-*a*]pyrimidinium iodide (**13-N**): 99% yield. For **13-F**: ¹H NMR (CDCl₃) δ 2.70 (s, 3H), 2.77 (s, 3H), 3.10 (s, 3H), 3.28 (s, 3H), 4.13 (s, 3H), 7.34 (s, 1H). For **13-N**: ¹H NMR (CDCl₃) δ 2.77 (s, 3H), 2.83 (s, 3H), 3.13 (s, 3H), 3.28 (s, 3H), 4.13 (s, 3H), 7.22 (s, 1H). The ratio of **13-N** and **13-F** was 2:1.

2,4,12-Trimethyl-6 λ^4 -pyrido[1'',2'':2',3'][1,2,4]-thiadiazolo[1',5':1,5][1,2,4]thiadiazolo[2,3-*a*]pyrimidinium iodide (**14-F**) and **2,4,13-trimethyl-6 λ^4 -pyrido[1'',2'':2',3']**[1,2,4]-thiadiazolo[1',5':1,5][1,2,4]thiadiazolo[2,3-*a*]pyrimidinium iodide (**14-N**): 53% yield. For **14-F**: ¹H NMR (CDCl₃) δ 2.74 (s, 3H), 3.26 (s, 3H), 4.16 (s, 3H), 7.58 (t, *J* = 6.0 Hz, 1H), 7.70 (t, *J* = 8.6 Hz, 1H), 8.26 (t, *J* = 8.6 Hz, 1H), 9.82 (d, *J* = 6.0 Hz, 1H). For **14-N**: ¹H NMR (CDCl₃) δ 2.64 (s,

3H), 3.15 (s, 3H), 4.10 (s, 3H), 7.07 (s, 1H), 7.52 (t, *J* = 6.2 Hz, 1H), 7.84 (d, *J* = 8.4 Hz, 1H), 8.14 (t, *J* = 8.4 Hz, 1H), 10.29 (d, *J* = 6.2 Hz, 1H). The ratio of **14-N** and **14-F** is 9:1.

2,10,12-Trimethyl-6 λ^4 -pyrido[1'',2'':2',3'][1,2,4]thiadiazolo[1',5':1,5][1,2,4]thiadiazolo[2,3-*a*]pyrimidinium iodide (**11a**): 76% yield; mp 285 °C dec; ¹H NMR (CDCl₃) δ 2.58 (s, 3H), 2.61 (s, 3H), 4.07 (s, 3H), 7.18 (d, *J* = 6.3 Hz, 1H), 7.20 (d, *J* = 5.4 Hz, 1H), 7.46 (s, 1H), 7.53 (s, 1H), 9.09 (d, *J* = 5.4 Hz, 1H), 9.40 (d, *J* = 6.3 Hz, 1H).

12-Ethoxycarbonylmethyl-2,10-dimethyl-6 λ^4 -pyrido[1'',2'':2',3'][1,2,4]thiadiazolo[1',5':1,5][1,2,4]thiadiazolo[2,3-*a*]pyrimidinium iodide (**11b**): 88% yield; mp 225–226 °C; ¹H NMR (CDCl₃) δ 1.32 (t, *J* = 7.2 Hz, 3H), 2.56 (s, 6H), 4.30 (q, *J* = 7.2 Hz, 2H), 5.49 (s, 2H), 7.0–7.3 (m, 2H), 7.53 (bs, 2H), 8.90 (d, *J* = 5.9 Hz, 1H), 9.37 (d, *J* = 6.4 Hz, 1H).

General Procedure for Preparation of 13-F and 14-N. A mixture of 2-(methylamino)-4,6-dimethylpyrimidine (**15**, 120.3 mg, 0.88 mmol) and 4,6-dimethyl-2-isothiocyanatopyrimidine **6a** in chloroform (3 mL) was heated at reflux temperature for 10 h. Removal of solvent gave thiourea (175.4 mg). A mixture of the solid product (63.4 mg) and NCS (26.7 mg, 0.20 mmol) in chloroform (4 mL) was stirred at room temperature for 20 min. Filtration of the mixture afforded a solid product. The solid was treated with KI to give **13-F**.

3-Chloro-2,4,8,10,12-pentamethyl-6 λ^4 -pyrimido[1'',2'':2',3'][1,2,4]-thiadiazolo[1',5':1,5][1,2,4]thiadiazolo[2,3-*a*]pyrimidinium iodide (**13-F**): ¹H NMR (CDCl₃) δ 2.70 (s, 3H), 2.77 (s, 3H), 3.10 (s, 3H), 3.28 (s, 3H), 4.13 (s, 3H), 7.34 (s, 1H).

2,4,13-Trimethyl-6 λ^4 -pyrido[1'',2'':2',3'][1,2,4]thiadiazolo[1',5':1,5][1,2,4]thiadiazolo[2,3-*a*]pyrimidinium iodide (**14-N**): ¹H NMR (CDCl₃) δ 2.64 (s, 3H), 3.15 (s, 3H), 4.10 (s, 3H), 7.07 (s, 1H), 7.52 (t, *J* = 6.2 Hz, 1H), 7.84 (d, *J* = 8.4 Hz, 1H), 8.14 (t, *J* = 8.4 Hz, 1H), 10.29 (d, *J* = 6.2 Hz, 1H).

Preparation of 12-*d*₆ from Deuterated 2-Methylamino-4,6-dimethylpyrimidine (15-*d*₆). To deuterium oxide (5 mL) was slowly added 94.2 mg of NaH (62.3% in oil). To the resultant aqueous NaOD solution was added **15** (113.4 mg, 0.83 mmol), and the solution was heated at reflux temperature for 1 h. The deuterated compound was extracted into ether, and the organic layers were concentrated to give 109.4 mg of **15-*d*₆**. Deuterated 10-S-3 sulfurane **12-*d*₆** was prepared by a similar procedure to that used in the preparation of **13-F**. The ¹H NMR spectrum of the sample in D₂O indicated that two methyl groups at 8,10-positions of **12** were 95%-enriched: ¹H NMR (CDCl₃) for **12-*d*₆** δ 2.73 (s, 3H), 3.03, 3.20 (d, *J* = 0.66 Hz, 3H), 4.11 (s, 3H), 7.16 (s, 1H), 7.30 (s, 1H).

***N,N*'-Di(4,6-dimethyl-2-pyrimidinyl)-*N,N*'-dimethylthiourea (16).** To a mixture of 2-(methylamino)-4,6-dimethylpyrimidine (**15**, 1.31 g, 9.6 mmol) and sodium hydrogen carbonate (880 mg, 10 mmol) in 55 mL of acetonitrile was added thiophosgene (0.37 mL, 4.9 mmol), and the mixture was heated at reflux temperature for 12.5 h. The mixture was poured into water, and the product was extracted into dichloromethane. The organic layers were dried over Na₂SO₄ and concentrated to leave a solid residue. Column chromatographic separation of the solid on silica gel (*n*-hexane:ethyl acetate = 2:1) afforded **16**. Recrystallization from methanol gave **16** as a pure sample: 43% yield; mp 168–170 °C; ¹H NMR (CDCl₃) δ 2.15 (s, 12H), 3.83 (s, 6H), 6.26 (s, 2H).

2,4,8,10,12,13-Hexamethyl-6 λ^4 -pyrimido[1'',2'':2',3'][1,2,4]thiadiazolo[1',5':1,5][1,2,4]thiadiazolo[2,3-*a*]pyrimidinium Di(triiodide) (**17**). A mixture of **16** (53.4 mg, 0.17 mmol) and iodine (129 mg, 0.51 mmol) in dichloromethane (20 mL) was stirred for 30 min at room temperature to afford precipitates. The resultant precipitates were obtained by filtration and recrystallized from acetonitrile to give 180 mg (99%) of **17**: mp 156–157 °C dec; ¹H NMR (CD₃CN) δ 2.83 (s, 6H), 2.99 (s, 6H), 4.57 (s, 6H), 7.66 (s, 2H); ¹³C NMR (acetone-*d*₆) δ 19.77, 25.97, 40.07, 122.45, 151.40, 162.05, 178.31, 210.46; UV (CH₃CN) λ_{\max} nm (ϵ) 362 (49 400), 292 (106 000), 238 (29 400).

General Procedure for Preparation of 18a,b via 19a,b, 20a,b, and 21a,b. A mixture of *N*-ethylaniline (2.0 g, 19 mmol) and 4,6-dimethyl-2-isothiocyanatopyrimidine (**6a**, 1.5 g, 9 mmol) in 10 mL of acetonitrile was stirred at room temperature for 20 h. The mixture was filtered, and the solid was recrystallized from methanol to give a pure sample **19** (550 mg) in 97% yield. To a solution of **19** (50 mg, 0.17 mmol) in dichloromethane (3 mL) was added SO₂Cl₂ (0.015 mL, 0.19 mmol) at 0 °C. After stirring overnight, 140 mg (1.7 mmol) of

sodium hydrogen carbonate was added to the reaction mixture to afford precipitates. The resultant precipitates were filtered, and the filtrate was concentrated to give a residue. Column chromatographic separation of the residue on silica gel (ethyl acetate) gave a solid product (40 mg). Recrystallization of the solid from dichloromethane-*n*-hexane afforded **18** as a pure sample.

1-Methyl-2-[2'-(4',6'-dimethylpyrimidinyl)imino]benzothiazoline (18a): 84% yield; mp 194–195 °C; ¹H NMR (CDCl₃) δ 2.54 (s, 6H), 3.90 (s, 3H), 6.66 (s, 1H), 7.19–7.61 (m, 4H).

1-Ethyl-2-[2'-(4',6'-dimethylpyrimidinyl)imino]benzothiazoline (18b): 83% yield; mp 168–169 °C (dichloromethane-*n*-hexane); ¹H NMR (CDCl₃) δ 1.42 (t, *J* = 7.1 Hz, 3H), 2.54 (s, 6H), 4.53 (q, *J* = 7.1 Hz, 2H), 6.65 (s, 1H), 7.18–7.61 (m, 4H).

Alternative Synthesis of 18b. To a suspension of *N*-ethyl-2-chlorobenzothiazolium tetrafluoroborate²³ (**23**) (768 mg, 2.7 mmol) in dichloromethane (10 mL) was added a solution of 2-amino-4,6-dimethylpyrimidine (**5a**, 917 mg, 7.5 mmol) in dichloromethane (10 mL) at 0 °C. After the mixture was stirred for 5 h at room temperature, sodium hydrogen carbonate (230 mg, 2.7 mmol) was added. The mixture was filtered, and the filtrate was concentrated followed by column chromatographic separation on silica gel (ethyl acetate) to give a solid product. Recrystallization from dichloromethane-*n*-hexane afforded **18b** as a pure sample (104 mg) in 14% yield.

Methylation of 18b: 1-Ethyl-2-[2'-(1,4,6-trimethylpyrimidinylimino)benzothiazoline Tetrafluoroborate (22). To a solution of **18b** (97 mg, 0.34 mmol) was added methyl iodide (0.09 mL, 1.5 mmol) at room temperature. The mixture was stirred overnight at the same temperature to afford precipitates. The solid product was obtained by filtration and was dissolved into acetonitrile (20 mL). To the solution was added silver tetrafluoroborate (90 mg, 0.46 mmol). The resultant solid product was recrystallized from acetonitrile to give **22** as a pure sample: 95% yield; mp 190 °C dec; ¹H NMR (CD₃CN) δ 1.47 (t, *J* = 7.2 Hz, 3H), 2.64 (s, 3H), 2.68 (s, 3H), 3.98 (s, 3H), 4.64 (q, *J* = 7.2 Hz, 2H), 7.07 (s, 1H), 7.45–7.92 (m, 4H).

1-Ethyl-*N*-methyl-2-[2'-(4',6'-dimethylpyrimidinyl)imino]benzothiazolinium Tetrafluoroborate (24). To a suspension of **23** (488 mg, 1.7 mmol) in dichloromethane (5 mL) was added a solution of 2-(methylamino)-4,6-dimethylpyrimidine (**15**, 704 mg, 5.1 mmol) in dichloromethane (5 mL) at 0 °C. After the mixture was stirred for 5 h at room temperature to give precipitates, the solid product was recrystallized from dichloromethane. To a solution of the chloride salt in dichloromethane was added silver tetrafluoroborate (340 mg, 1.7 mmol). The mixture was stirred at room temperature overnight. The mixture was filtered, and the filtrate was concentrated to give the solid product. Recrystallization of the solid from dichloromethane-*n*-hexane gave **24** (228 mg) as a pure sample in 47% yield: mp 175 °C; ¹H NMR (CDCl₃) δ 1.52 (t, *J* = 7.2 Hz, 3H), 2.16 (s, 6H), 3.88 (s, 3H), 4.51 (q, *J* = 7.2 Hz, 2H), 7.03 (s, 1H), 7.73–8.12 (m, 4H).

Kinetic Measurement on Deuterium Exchange. General Procedure. A solution of **8a** (1.94 mg, 6.8 × 10⁻³ mmol) in methanol-*d*₄ (0.5 mL) was placed in a 5-mm NMR tube. The tube was immersed in a constant-temperature bath maintained at 80 °C. After a measured amount of time, the tube was removed from the bath and immediately cooled in an ice-water bath at each interval, the ¹H NMR spectra (400 MHz) of the methyl region were recorded, and the relative integrated areas of the peaks were used to calculate the percent composition of the starting material and the resultant deuterated sample. The values of the pseudo-first-order rate constant, *k*, for the deuteration were calculated by using the method of least squares. The kinetic measurements for the other substrates (**9b**, **12**, and **18b**) were done by the same procedure. The results are summarized in Table 3.

Measurements of the Restricted Rotational Energy Barriers for the 10-S-3 Sulfuranes 8a–i, 9a–d, 9f, and 12. Line Shape Calculations. The theoretical NMR line shapes were calculated according to an analytical expression, which was originally developed by Gutowsky et al. in a classical treatment that incorporated nuclear site exchange into the solutions of the Bloch equations.^{12,24}

The rate constants for various temperatures were obtained by visually matching observed and calculated spectra. Activation energies were obtained from plots of ln(*kNh*/RT) vs 1/*T*, where *N* is 6.02 × 10⁻²³, *h* = 1.58 × 10⁻³⁴ cal·s, and *R* = 1.987 cal·mol⁻¹·K⁻¹. The plots were linear over the temperature range. These Eyring plots give slopes of -Δ*H*[‡]/*R* and *y*-intercept values of Δ*S*[‡]/*R*.

Coalescence Temperature Method. The two methyl signals of **8a–i**, **9a–f**, and **12** coalesced at each temperature in various solvents, respectively. The exchange rate at the coalescence temperature was calculated by using the Gutowsky–Holm approximation (*kc* = πΔ*ν*/√2) and the Δ*G*_c[‡] value by using the Eyring equation, assuming a transmission coefficient of unity.¹²

X-ray Crystallographic Analysis. A colorless crystal of **8a**, that of **9a**, and a black brown crystal of **17** were mounted on a glass fiber at room temperature. The data were collected on a Mac Science MXC³ diffractometer using Mo Kα radiation with a graphite monochromator. Lattice parameters were determined by least-squares fitting of 31–45 reflections with 22 < 2θ < 31, 31 < 2θ < 38, and 6 < 2θ < 29 for **8a**, **9a**, and **17**, respectively. Data were collected with ω-scan mode. All data were corrected for absorption²⁵ and extinction;²⁶ in addition data for **9a** were corrected for the observed linear decay of the reference reflections. The structures were solved by a direct method with the program Monte Carlo–Multan.²⁷ Refinement of F was carried out by full-matrix least squares. All non-hydrogen atoms in **8a**, **9a**, and **17** were refined with anisotropic thermal parameters. All hydrogen atoms could be found on a difference Fourier map; these coordinates were included in the refinement with isotropic thermal parameters. All the computations were carried out on a Titan-750 computer.

The structures were solved by direct methods and refined by full-matrix least-squares methods. Neutral atom scattering factors and anomalous scattering correction terms were taken from the international Tables for X-ray Crystallography. Full details about crystal data and refinement are presented in Table S4 (supporting information).

Calculation. Calculation of energy levels, formal charge, and bond population were carried out with use of standard AM1 procedure from the MOAPAC version 3.0.^{21,28} All calculations were based on experimental geometries determined by the X-ray crystallographic analysis.

Acknowledgment. We are indebted partially to a Grants-in-Aids for Scientific Research (No. 03453029) administered by the Ministry of Education, Science, and Culture of the Japanese Government. We also thank Dr. Yohsuke Yamamoto of Hiroshima University for X-ray crystallographic studies and Dr. Satoshi Yabushita of Keio University for his advice on the AM1 calculations.

Supporting Information Available: Characterization data for **6f–j**, **7a–p**, **8a–i**, **9a–f**, **10**, **11a,b**, **12**, **13-F**, **14-N**, **16**, **17**, **18a,b**, **22**, and **24** are described, including satisfactory analytical data (0.4% for C, H, and N) for new compounds. Four tables on kinetic data not listed in Table 1 (Table S1), density matrixes (Table S2), and coefficients (Table S3) for MO around the sulfur atom in **8a** and **17** as well as complete crystallographic data (Table S4) and structural data (bond lengths and angles and atomic coordinates) for **8a**, **9a**, and **17** are added (51 pages). See any current masthead page for ordering information and Internet access instructions.

JA952591C

(24) Gutowsky, H. S.; McCall, D. W.; Slichter, C. P. *J. Chem. Phys.* **1953**, *22*, 279.

(25) Furusaki, A. *Acta Crystallogr.* **1979**, *A35*, 220.

(26) Katayama, C. *Acta Crystallogr.* **1986**, *A42*, 19.

(27) Coppens, P.; Hamilton, W. C. *Acta Crystallogr.* **1970**, *A26*, 71.

(28) (a) Stewart, J. J. P. *QCPE Bull.* **1983**, *3*, 43. (b) Dewar, M. J. S.; Zoebisch, E. G. *J. Mol. Struct. (THEOCHEM)* **1988**, *180*, 1.

(23) Balli, H.; Kersting, F. *Ann.* **1961**, *647*, 1.